Sensors and Actuators Reports 4 (2022) 100100

Contents lists available at ScienceDirect

Sensors and Actuators Reports

journal homepage: www.sciencedirect.com/journal/sensors-and-actuators-reports

A review on chemiresistive ZnO gas sensors

Mariane A. Franco [a,b], Patrick P. Conti [c], Rafaela S. Andre [a], Daniel S. Correa [a,b,*]

[a] Nanotechnology National Laboratory for Agriculture (LNNA), Embrapa Instrumentation, São Carlos, SP 13560-970, Brazil
[b] PPGQ, Department of Chemistry, Center for Exact Sciences and Technology, Federal University of São Carlos (UFSCar), São Carlos, SP 13565-905, Brazil
[c] Institute of Molecular Chemistry and Materials/Charles Gerhardt Montpellier Institute, University of Montpellier, Place E. Bataillon, Montpellier Cedex 05, 34095, France

ARTICLE INFO

Keywords:
Chemiresistive sensors
ZnO
Heterojunction
Gas sensors
Hybrid materials
Composites

ABSTRACT

Chemiresistive gas sensors have been widely applied to monitor analytes of environmental, food and health importance. Among the plethora of materials that can be used for designing chemiresistive sensors, ZnO is one of the most explored for gas sensing, as this material has a low-cost, is non-toxic and can be easily obtained through standard chemical synthesis. Adding to this, ZnO can form heterostructures capable to improve sensor performance regarding sensitivity, selectivity and stability. Moreover, ZnO heterostructures also contribute to lower operating temperature of gas sensors, since the synergistic effects contribute to amplify the sensor signal. In this review, we survey recent advances on different types of chemiresistive ZnO-based gas sensors, focusing on how the morphology and structure of these materials influence on the sensor response. Challenges and future perspectives for ZnO chemiresistive sensors are also discussed.

1. Introduction

The continuous increase in human activities resulting in high level of pollution, combined to the modern lifestyle that integrates gadgets for all sorts of activities monitoring, have increased the demand for sensing devices. For instance, food processing and air quality monitoring are only a few of the vast areas in need for reliable and efficient sensors [1–7]. In this direction, several sensing devices have been designed and exploited in order to meet the demands of modern society, with emphasis on chemiresistive sensors. These devices employ materials that can detect changes in their environment based on changes in their electrical properties [8–10]. The term was first employed in 1985 by Wohltjen et al [11], who developed a copper phthalocyanine-based sensor for ammonia detection. Over the years, semiconducting metal oxides (SMO) [12], polymers [13], metallic nanoparticles [14] and other materials have also been applied in the development of chemiresistive sensors.

Owing to their low production cost, easy processability, chemical versatility and good electrical properties, several SMOs, including CdO [15,16], In_2O_3 [17,18], Fe_2O_3 [19,20], WO_3 [21,22], SnO_2 [23–25], CuO [26,27], TeO_2 [28], MoO_3 [29,30] and ZnO [31,32], have been successfully explored in chemiresistive sensors. ZnO, an n-type semiconductor with direct band-gap at room temperature, presents prominent importance once it has high electron mobility, thermal stability, and good electrical properties for gas sensing applications [33,34]. Besides, ZnO has oxygen molecules adsorbed onto its surface, which can form ionized species capable to capture electrons from the conducting band of the oxide, creating a depletion layer at the oxide surface [35]. These appealing features prompt ZnO to be vastly exploited in the design of chemical sensors. Besides, in order to optimize the material's properties for chemical sensors, the control and creation of new morphologies, shapes and crystallographic phases of ZnO have been highly explored. Although some recent works have surveyed ZnO sensors, most of them concern to a general view considering ZnO sensors in particular aspects such as temperature of operation, specific type of morphology or yet different transduction method from this review [36–38]. This review presents a recent survey on ZnO-based chemiresistive sensors fabricated using varied morphologies, such as 0D (quantum dots - QDs), 1D (nanorods, nanoribbons, nanotubes, nanofibers and nanowires), 2D (nanosheets and nanofilms) and 3D (nanoflowers, porous spheres and hollow spheres) nanomaterials, as schematically illustrated in Scheme 1. The focus is to present to the reader how the distinct morphologies and structures/heterostructures of ZnO composing the chemiresistive sensors can influence the final sensor performances towards varied analytes.

* Corresponding author.
E-mail address: daniel.correa@embrapa.br (D.S. Correa).

https://doi.org/10.1016/j.snr.2022.100100
Received 20 January 2022; Received in revised form 26 March 2022; Accepted 4 April 2022
Available online 10 April 2022

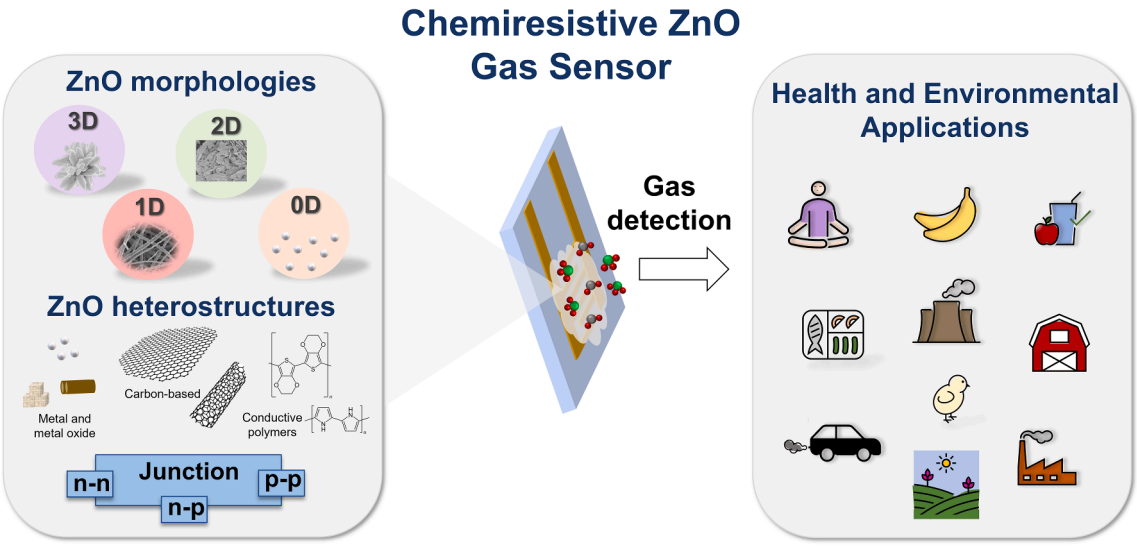

Scheme 1. An overview of the ZnO morphology and heterostructure junction types for improved chemiresistive gas sensor response.

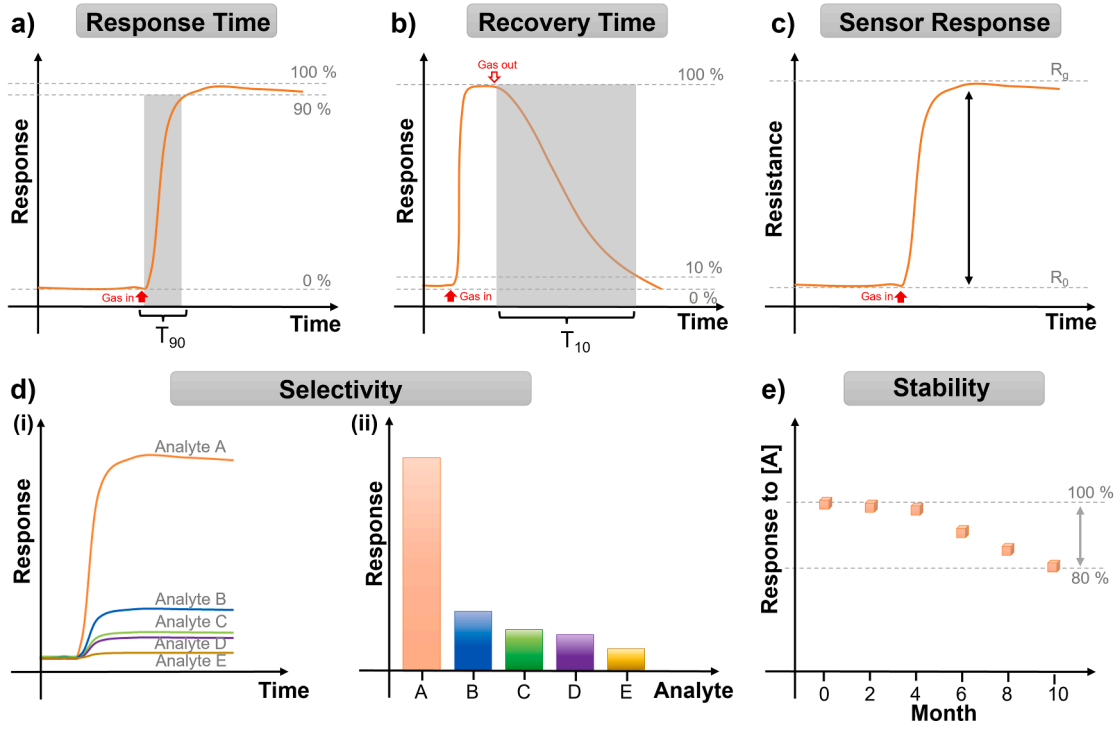

Fig. 1. Graphical representation of (a) response time, (b) recovery time, (c) sensor response, (d) selectivity ((i) and (ii)) and (e) sensor stability.

2. *Chemiresistive gas sensors: factors influencing the sensor performance*

The sensor performance is dependent of a few parameters such as response time, recovery time, sensing response, selectivity, limit of detection and stability. Next, we present an overview of these parameters considering their characteristics and particularities. Besides, the sensors' figure of merit are graphically represented in Fig. 1.

2.1. *Response time*

This parameter measures the time taken by the sensor to provide a response after exposure to the analyte. Usually, a percentage of sensor response is used to determine this parameter, reported as the time to reach 90% of its maximum response (T_{90}), as represented in Fig. 1a [39, 40]. This parameter can be very important for understanding sensor performance, as it helps to understand the kinetics and magnitude of the interaction between the sensing layer and the target gas. However, this variable can be affected by external stimuli such as temperature, gas concentration and flow rate within an experiment [41–43].

2.2. *Recovery time*

The recovery time describes the opposite process of the response time. It concerns the time required by the sensor to return to the original baseline response when the target analyte is removed and the sensor has contact with pure carrying gas, usually air or nitrogen [44]. It is not

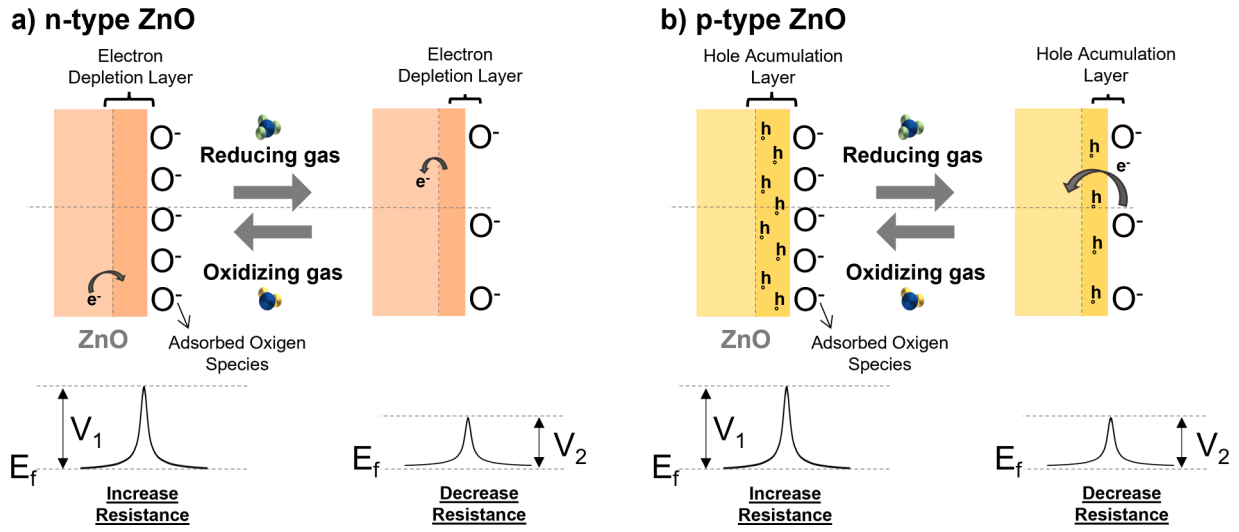

Fig. 2. Schematic representation of sensing mechanism for (a) pristine n-type ZnO and (b) pristine p-type ZnO exposed to reducing gases (right side of each representation) and oxidizing gases (left side of the representation). Under each scheme, there is the potential barriers representation before and after exposure indicated as V_1 and V_2, respectively.

uncommon to find articles using the term T_{10}, which is the time required to achieve a recovery of 90% (Fig. 1b) [39,40].

2.3. Sensor response

The sensor response of chemiresistive sensors can be defined as the change caused on the electrical behavior of the sensing devices exposed to the analyte (Fig. 1c). This parameter calculated by different forms, usually involving the ratio of electrical behavior prior and posterior to gas exposure according with gas analyte reducing/oxidizing behavior. For example, for reducing gases the response can be considered as R_0/R_g and for oxidizing gases as R_g/R_0, where R_0 is the sensor electrical behavior in reference gas (usually air) and R_g the sensor electrical behavior when exposed to the target gas. Besides, the response percentage can be obtained from the expression $[(R_0 - R_g)/R_0] * 100\%$.

2.4. Sensitivity

The sensitivity is another important parameter for evaluating sensor performance. Usually is represented by S and can be defined as the ratio of sensor response/gas concentration. In other words, the sensitivity is a measure of how much change a specific amount of analyte can cause to the sensor and can be estimated by the slope of a sensor's calibration curve.

2.6. Selectivity

It's usually defined as the tendency of the sensor to discriminate an electrical response for a target gas in the presence of other gases under the same conditions (Fig. 1d). Selectivity can be mathematically defined as the ratio between the responses of a target gas and the responses to an interferent [45]. Besides, the graphical representation can be in terms of dynamic curve of sensor response or bar charts of sensor response for target analyte and interferents.

2.7. Stability

This parameter considers the period of time that the sensor platform will retain the same performance regarding the electrical response when exposed to certain analyte in the same conditions. In Fig. 1e, the hypothetical stability is 4 months. The stability can vary from days up to months [46].

2.8. Limit of detection (LOD)

The LOD can be defined as the minimum concentration of analyte that can be identified by the sensor under specific operating conditions. Usually, it might be simply determined by a signal to noise ratio greater than 3 (LOD = 3 S/N, where S is standard deviation of the response and N the slope of calibration curve). Given the real concentrations of toxic gases, it is desirable that sensors can operate in low concentration ranges [47].

To improve the performance of chemiresistive sensors, heterojunctions can be used, which consist in the physical interface between two different materials, such as p type like materials (CuO, NiO, CeO_2, Mn_2O_3, Co_3O_4, La_2O_4, Y_2O_3, Bi_2O_3, Ag_2O, TeO_2, Sb_2O_3 and CrO_3) and type n (ZnO, SnO_2, TiO_2, In_2O_3, MoO_3, MgO, Al_2O_3, Ga_2O_3, Nb_2O_5, ZrO_2, CaO, V_2O_5, Ta_2O_5 and WO_3) materials [48–50]. By producing intimate electrical contact at the interface between two different materials, Fermi levels balanced with the same energy result in charge transfer and the formation of a charge depletion layer, leading to better performance of the sensor [51–54]. With both interfaces exposed to the atmosphere, additional anomalies can happen as they have two different semiconductor materials in close proximity. A gas or liquid can react more readily with one material producing a by-product that can react with the second material to complete the reaction, known as a synergistic reaction. Nano-heterostructures are often used in gas sensors, as their small dimensions and high surface-to-volume ratio lead to improvements in the effects [48–50]. Doping oxides can also be used to control the microstructure and morphology of the material during processing [48]. Although manipulation of the microstructure is often the claim to improved performance, electronic and chemical effects also play a role. The improvements in the detection performance of these compounds have been attributed to many factors, including electronic effects, such as: band flexion due to the Fermi level balance [55,56], separation of the loader [57], manipulation of the depletion layer [58–60] and increased barrier energy of interfacial potential [61]; chemical effects, such as decreased activation energy [62], targeted catalytic activity [63] and synergistic surface reactions [64]; and geometric effects, such as grain refinement [65], increased surface area [66] and increased accessibility to gas [67].

3. Chemiresistive ZnO sensing mechanism

When ZnO chemiresistive sensor are exposed to distinct atmosphere

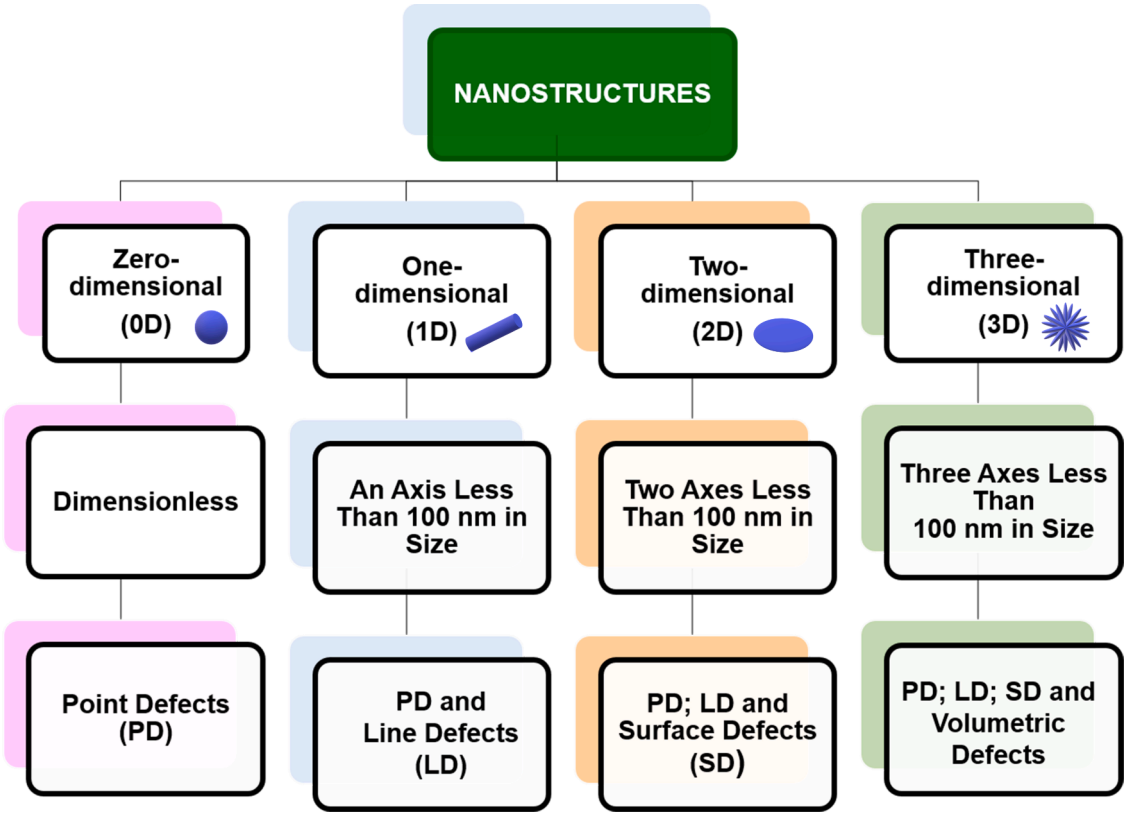

Fig. 3. Relationship between 0D morphologies; 1D; 2D and 3D with the defects found in the crystal lattice of nanostructures.

composition, changes in conductance and working function will be observed [36,68,69]. Such behavior is a result of the gas adsorption/-desorption to and from the ZnO surface, macroscopically speaking, and of the charge carries availability, microscopically speaking, forming the electron depletion layer, as illustrated in Fig. 2a. This mechanism is referenced as adsorption/desorption mechanism and can be modeled based on surface chemical or physical interaction [49]. Although the great majority of works explores the oxygen (chemical) adsorption/desorption mechanism, recent works have proven the chemical interaction of gas analyte with chemiresistive metal oxides other than ZnO [70]. Additionally, here we present oxygen adsorption/desorption mechanism followed by the general chemical and physical types of adsorption/desorption able to result in chemiresistive sensing response.

It is expected that ZnO nanostructures in air have oxygen molecules adsorbed onto their surface (Fig. 2 a), capturing electrons from ZnO conduction band and forming ionic oxygen species such as O_2^-, O^- and O^{2-} [71,72]. For n-type ZnO, the interaction between oxygen and ZnO conduction band electrons will lead to an electron depletion layer formation with high potential barriers, represented by V1 in Fig. 2. This high potential barrier hinders the charge carrier's movement over neighbor crystal grains. For p-type ZnO, this interaction leads to a hole accumulation layer, decreasing the resistance. Eventually, the oxygen species adsorption reaches equilibrium and microscopical properties such as conductance and working function are kept constant. The electrical resistance can be modulated to a maximum value by controlling ZnO thickness to be smaller than two times the Debye length (LD) extending the electron depletion layer over the entire material [73]. Considering n-type ZnO exposure to reducing gases, such as H_2S, H_2 and C_2H_5OH, the sensing mechanism that takes place is based on the analyte interaction with the ionic oxygen species that will be oxidized, releasing electrons back to ZnO conduction band [37,49,73]. Besides the electrons returning to ZnO conduction band, depletion layer thickness is reduced, the density of free charge carrier is increased, increasing the ZnO conductance and so decreasing ZnO electrical resistance [74]. By returning the ZnO to atmospheres without the reducing gas, the gas desorption step initiates and the oxygen species returns to ZnO surface increasing the resistance. Sensor responses based on this type of mechanism are usually reversible with fast recovery [73,74]. Furthermore, reducing gases interacting with adsorbed oxygen onto p-type ZnO will result in decreased resistance (Fig. 2b). On the other hand, n-type ZnO exposed to oxidizing target gases, such as SO_2, NOx and O_3, will present a decrease of free charge carriers' density once oxidizing gases adsorbs onto ZnO surface along with oxygen species capturing further electrons and so increasing the electrical resistance. While for p-type ZnO, oxidizing gases will increase the resistance thanks to the analyte interaction with adsorbed oxygen species which will release electrons back to ZnO, enlarging the hole accumulation layer and increasing the resistance [37].

Direct chemical interactions between the gas analyte and ZnO nanostructure are expected to occur only with oxygen species. For instance, H_2S detection by metal oxide SnO_2 has been was carefully investigated, revealing the formation of SnS_2 after SnO_2 exposure to the gas, indicating that H_2S developed close interaction reacting with the metal oxide [70].

Physical adsorption/desorption occurs through intermolecular forces and hydrogen bonding. Although physical adsorption/desorption is a common phenomenon, the change in conductivity caused by physical adsorption/desorption can be considered negligible and is rarely applied to elucidate the gas sensing mechanism [73].

Yet for increased temperatures, the ZnO sensing ability will be determined by the gas diffusion process as well as by the adsorbed oxygen species and structural porosity (for gas percolation) [69,75].

4. Zinc oxide

ZnO is a semiconductor (Group II-VI) displaying a broad band gap (around 3.4 eV), a high exciton binding energy (~60 meV), high

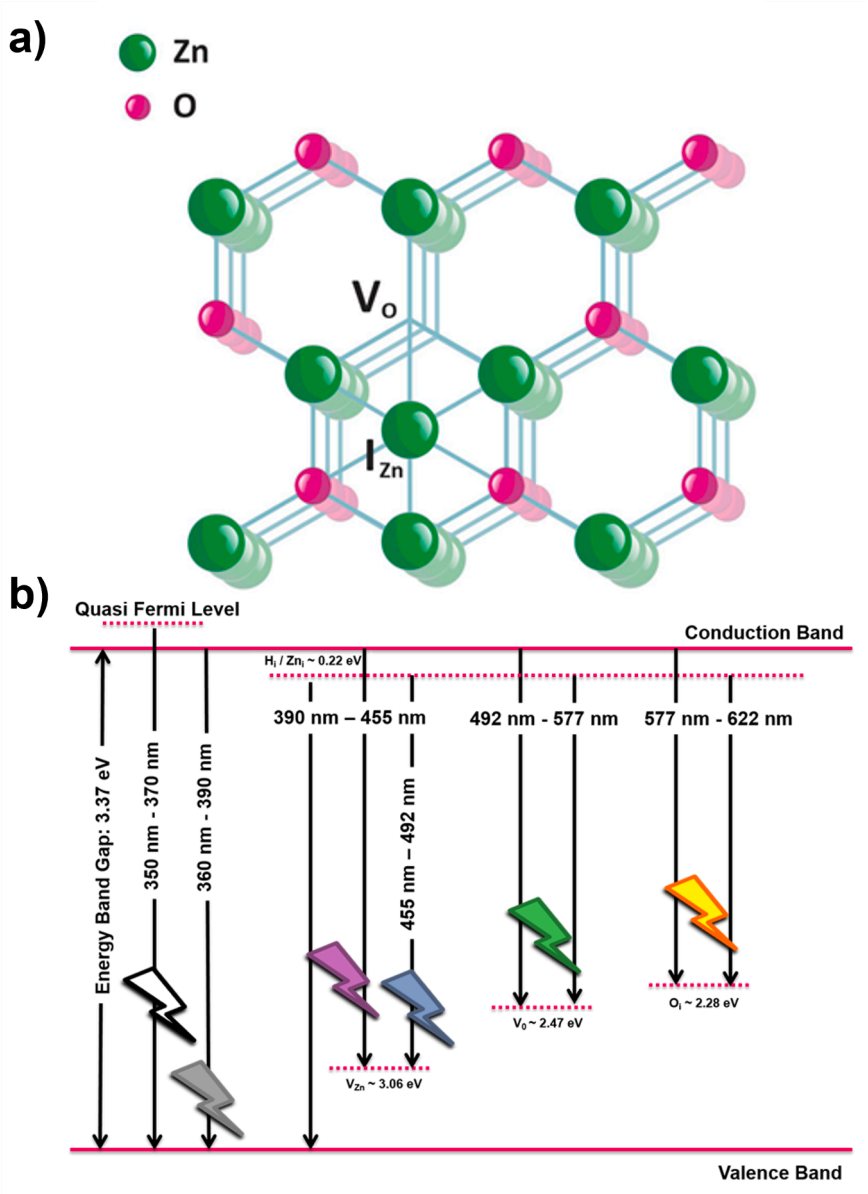

Fig. 4. (a) Point defects in the ZnO crystal lattice. Reprinted with permission from Ref. [88]. (b) Schematic energy level diagram of various defect level emissions in ZnO. Reprinted with permission from Ref. [84].

electron mobility 200 cm^2/V.s, excellent chemical and thermal stability and photoelectric response, which make this material a promising choice for gas sensor [43,76–80]. In addition, these materials are highly attractive, as they can be easily produced by chemical synthesis routes, are non-toxic, and low cost enabling mass production [43,76–80]. It is a highly versatile material that can be easily obtained as nanowire, nanorods, nanobelts, nanosprings, nanocombs, nanoplates, nanoneedles, nanoribbons, nanotubes, nanorings, nanoplates, nanopellets, nanoflowers, snowflakes, dandelion and coniferous urchin-like [81–83] for a optoelectronic, sensing and biomedical applications. These morphologies can be obtained by different synthesis processes, such as thermal evaporation, carbothermal reduction, magnetron sputtering, cathodic electrodeposition, hydrothermal synthesis and sol-gel processing [84].

These nanostructures can be periodically organized in three different types of crystalline network, namely *Rocksalt* (obtained under high pressures), *Zinc Blend* (obtained from epitaxial growth on seed crystal with cubic structure), and *Wurtzite* (hexagonal close-packed structure with space group P63mc, easily obtained in ambient conditions) [85]. The crystal structures presented as well-defined crystalline arrangements exhibit structural defects of different natures. These defects might affect grain boundary properties, mechanical properties, electrical conductivity of the semiconductors and atomic diffusion processes. The defects present in the crystalline structures can be classified in four basic types: point defects (zero-dimensional), line defects (one-dimensional), surface defects (two-dimensional) and volumetric defects (three-dimensional), related to the morphologies of the nanostructures (Fig. 3). These defects are originated during the synthesis process, due to variation in temperature, pressure, solvent, concentration and synthesis time, which can affect the morphology of the nanostructure and thus modify the material's crystal lattice [86,87].

In ZnO the most common defects are point defects such as oxygen vacancy (V_O), interstitial zinc (I_{Zn}) (Fig. 4a), interstitial oxygen (I_O) [88,89,90,91], and even interstitial hydrogen (I_H). V_O, I_{Zn} and I_H are assumed as potential donors, and are found in low concentrations in n-type ZnO under thermal equilibrium, indicating that the conductivity is attributed to residual impurities, including H impurities with various atomic configurations, metastable shallow O-vacancy, and Zn interstitial

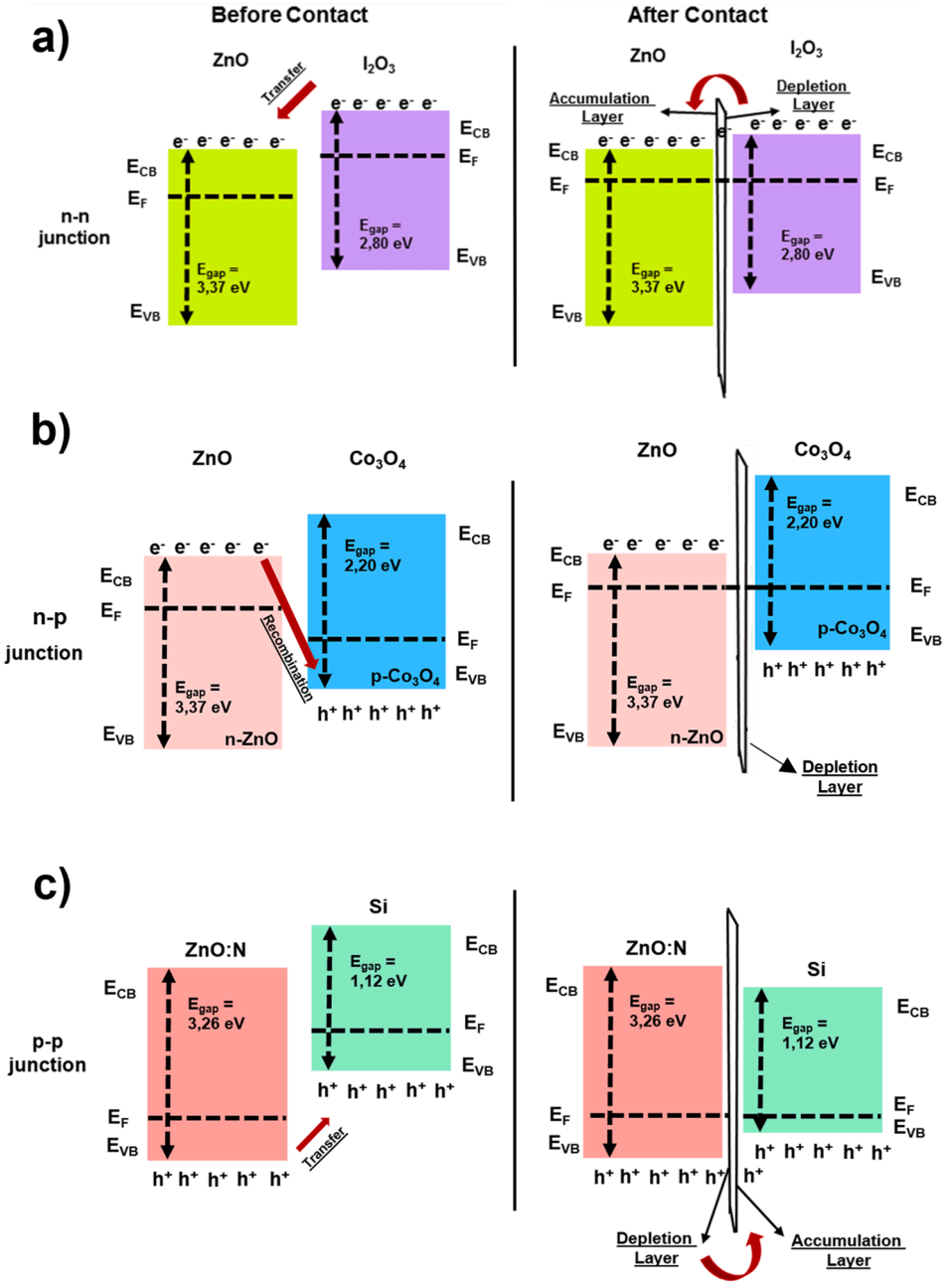

Fig. 5. Schematics representation of band bending at heterojunction; E_{VB}: valence band edge energy, E_F: fermi energy, E_{CB}: conduction band edge energy and E_{gap}: band gap energy. Adapted with permission from Ref. [48].

[92,93]. Zinc vacancy (V_{Zn}), oxygen interstitial (I_O) and anti-local oxygen (O_{Zn}) are assumed as possible acceptors, where the energy of defects formation suggests a preference for donor defects over acceptors, either for ZnO type n or type p [92,93]. In this way, point defects will generate surface defects in nanostructured ZnO influencing its final properties [82,94].

Thus, ZnO crystal lattice defects can be estimated, in general, by photoluminescence (PL) spectra that present emission bands in the ultraviolet (UV) regions centered at 380 nm, due to a band recombination and excitonic transition, and visible regions associated with intrinsic and extrinsic defects. Specifically, yellow-orange (577–622 nm) emissions can be attributed to interstitial oxygen, green emissions can be attributed to oxygen and zinc vacancies, and blue-violet emissions can be attributed to I_{Zn}, I_H and V_{Zn} (Fig. 4b) [89].

X-ray photoelectron spectroscopy (XPS) technique is another way to determine existing defects in ZnO nanostructures. This technique provides information on the chemical states of ZnO on the surface of the nanomaterial as well in the defects, complementing the PL technique [84]. For instance, it is well known that peaks in the ZnO XPS spectra around 530 eV are attributed to oxygen vacancies and at 1020 eV are attributed to interstitial zinc [84].

Considering ZnO-based chemiresistive sensors, generally the detection mechanism works by adsorption of the target species onto the oxide active sites such as adsorbed oxygen species and short-range structural defects. The adsorption of oxidizing gas molecules, such as SO_2, can remove and deplete electrons from the conduction band, resulting in a reduction in conductivity of ZnO chemiresistive sensor. On the other hand, reducing gas molecules such as CO can react with oxygen species adsorbed onto the surface, sharing electrons and increasing the conductivity [82].

4.1. Zinc oxide heterojunctions architectures

Despite the many interesting characteristics to be employed as gas sensors, ZnO requires high working temperatures to activate the adsorbed oxygen species and increase the reactivity towards the analyte gas. Besides, such high temperatures can decrease the sensor's stability [95] and lifetime [96], induce uncontrolled grain growth and limit the detection of flammables or explosive analytes [97]. Other drawback is the potential interference by water molecules present in the atmosphere, which can interact with ZnO through chemi- and physisorption processes [98]. In an attempt to mitigate these disadvantages towards gas sensing application, nanostructured ZnO, doped ZnO and ZnO heterostructures have been explored to increase sensitivity, selectivity and lower the operating temperature of the sensor. Regarding doping of ZnO, aluminum is perhaps the most common metal for this purpose, as it generates extra electrons and improves the optical, thermal, magnetic and electrical properties of ZnO [99]. Doped ZnO sensors are very selective, sensitive and stable and specific applications can be designed through careful selection of dopants [100,101]. The Fermi level for doped and intrinsic materials are close, due to the fixation of the Fermi level, making it difficult to transfer the charge carriers from the dopant to the semiconductor [102]. Unlike heterojunctions, the Fermi level of the two hybrid materials enter into equilibrium, with a greater charge transfer from one material to the other, avoiding the recombination of the electron-hole pairs and making many sensors working at temperature environment [48,103].

In general, ZnO heterostructures are obtained as nanocomposites, which might decrease the operating temperature, and improve the sensitivity, selectivity and stability of the sensor. Examples of nanomaterials usually combined with ZnO include CuO [104], NiO [105, 106], Co_3O_4 [107], WO_3 [108], SnO_2 [109], Fe_2O_3 [110], TiO_2 [111], SiO_2 [46,112], carbon-based materials such as graphene, reduced graphene oxide, graphene oxide and conjugated polymers as polypyrrole [113], polyaniline [114], poly(3,4-ethylenedioxythiophene) [115] and poly(3-hexylthiophene-2,5-diyl)) [116]. These composites can form heterostructures with: (i) n-n junction (Fig. 5a), where the available low-energy conduction band states (holes) stimulate electron transfer to n-ZnO; (ii) p-n junction (Fig. 5b) [48], where the available low-energy valence band states stimulate electron transfer across the interface [48], and (iii) when they are doped with p-type dopants [117] they can also form p-p junctions (Fig. 5c). Having holes as majority of the charge carriers, a region of depleted hole and accumulated hole is formed in p-doped zinc oxide and p-type nanomaterial, respectively. With this, under the influence of an applied potential, the electron-hole pairs formed by the internal electric field are separated, and the holes tend to flow to the negative field while electrons move to opposite direction (positive field), resulting in electron-hole pairs efficiently separated, enhancing sensing properties [118,119].

Another classification of heterostructures for metal oxides can be defined by the link between the energy bands of the constituent materials, namely type I, II and III, which correspond to straddling gap, staggered gap and broken gap [120,121].

For Type I heterojunction, the VB and CB of semiconductor A are lower and higher than the corresponding VB (valence band) and CB (conduction band) of semiconductor B, respectively. In this way, the generated electrons and holes transfer to the CB and VB of semiconductor B, which is negative for the separation of electron–hole pairs. Moreover, the redox reaction of the composite semiconductors with a type I heterojunction will conduct on the surface of semiconductor B with a lower redox potential and, thus, the redox ability of the photocatalyst may be suppressed [120,121]. For type II heterojunctions, the VB and CB of semiconductor A are higher than that of semiconductor B, thus the generated electrons will migrate from the CB of semiconductor A to that of semiconductor B with a lower reduction potential, and the corresponding holes in the VB of semiconductor B will migrate to semiconductor A with a lower oxidation potential. Thus, a spatial separation of electron–hole pairs will be completed. On the other hand, for type III heterojunctions the band gap of the two semiconductors will not overlap and, as a result, there is no transmission or separation of electrons and holes between semiconductor A and semiconductor B. Consequently, the type II heterojunction is the most effective structure for improving the gas sensor performance of semiconductors, and has received a great deal of research attention [120,121].

P-n heterojunction has been reported as the most efficient for the construction of sensitive, selective and stable gas sensors with short response time operating at ambient temperature for the analysis of gases [48]. Besides, the most reported morphology are based on one-dimensional (1D) structures, once they are very easy to be obtained, display large surface area to volume ratio and enable rapid charge transfer, enhancing the response time and sensitivity of resistive gas sensors [122]. Moreover, most heterojunctions based on ZnO are obtained in relative mild conditions through hydrothermal method using temperatures ranging from 100 to 200 °C under pressure, in addition to using water as solvent with adjustable pH [123–125]. For instance, ZnO-CuO heterostructures have attracted attention recently due to the high stability under exposure to several gases and optoelectronic properties [126,127]. Besides, ZnO-CuO are non-toxic, inexpensive cost of production, turning it in a featured alternative with suitable properties for application in gas sensors [126,127].

In addition to heterojunctions formed with inorganic materials, ZnO can also form heterostructures with organic compounds. For instance, in p-type organic semiconductors π electrons have a strong influence on the entire organic structure due to multiple intermolecular interactions, as well as suppressed molecular motions, resulting in two-dimensional (2D) charge transport packing structures [128]. On the other hand, n-type organic semiconductors have π-electron deficient nuclei and a flat and rigid molecular structure throughout the extended π-electron structure, promoting charge carrier transport via π-π intermolecular superposition in the solid state [128].

Apart from organic semiconductors, there are also some conductive carbon materials [129], such as carbon nanotubes and graphene, which are suitable for sensing applications, once they combine excellent detection and transduction properties at room temperature, where the conductivity is changed by very small amounts of adsorbed gas molecules. In short, the electrical resistance of carbon nanostructures is altered by the electron transfer between carbon nanostructures and oxidized or reduced gas molecules that are adsorbed onto their surface, being considered the main detection mechanism. Even though gas sensors based on carbon nanostructures have these advantages, they have certain limitations, such as irreversibility and long recovery time. One of the possibilities to improve the properties of these sensors is to use carbon materials/metal oxide (MOs) heterostructures in order to develop systems with suitable response at ambient temperature towards varied analytes. These materials are not just the sum of the individual components, but new compounds with new properties and functionalities. Some of the carbon nanostructures/MOs heterostructures mentioned have greater sensitivity to the target gas at room temperature than the individual materials [129]. These characteristics can also be observed in heterostructures with conductive metals/metal oxides [130–132].

According to the literature, ZnO combined with carbon compounds are more promising as gas sensors than those that are decorated with metals. This is possible due to the fact that metals have around one, two or three electrons in the valence band, forming the electronic cloud of the metal, while conductive carbon compounds, due to sp^2 hybridization, have delocalized π electrons, being bound to a greater number of carbon atoms by covalent bonding than metals in a metallic bond [133, 134]. Thus, the electron sea of these compounds is larger as well as it is the surface area, causing the working temperature of the sensor to decrease, and the sensitivity and selectivity to increase compared to metals. Besides, when conductive carbon compounds are confined to zero dimension (quantum dots), in addition to decrease the working

Table 1
An overview of ZnO-based gas sensors employing different morphologies.

Morphology	Synthesis method	Operating temperature /°C	Gas and concentration / ppm	Response (S)	Response time / s	Recovery time / s	Ref.
ZnO nanoparticles	Sol-gel method	350	H_2S / 150	~23 (1)	265	940	[139]
ZnO-Cr_2O_3				27 (1)	385	690	
ZnO nanoparticle	Hydrothermal reaction	350	Ethanol / 400	20.3 (2)	12	4	[140]
ZnO Nanoplates				23.3 (2)	23	5	
ZnO Nanoflowers				30.4 (2)	10	4	
ZnO QDs	Colloidal method	225	Formaldehyde	~15 (2)	5	9	[40]
		300	/ 50	~8.5 (2)	-	-	
		275	Toluene / 50	~6.5 (2)	-	-	
		200	Benzene / 50	~8 (2)	-	-	
			Ammonia / 50				
ZnO QDs	Colloidal method	120	H_2S / 68.5	~1700 (2)	-	-	[141]
ZnO nanorods	Precipitation reaction	219	Acetone / 100	12.9 (2)	13	29	[39]
Au-ZnO		172		50.5 (2)	1	20	
ZnO nanowires	Electrospinning technique	RT	NH_3 / 50	20 (2)	88	65	[142]
Ag-ZnO nanoneedles	Hydrothermal reaction	370	Acetone / 100	18.112 (2)	10	21	[143]
ZnO nanoneedles	VS and VL mechanism	195	NO_2 / 5	600% (3)	1050	840	[144]
		310	Benzene / 5	35% (3)	240	150	
		310	Formaldehyde	25% (3)	180	210	
			/ 5				
ZnO-U Nanofibers	Electrospinning technique / Oxygen-plasma treatment	250	Acetone / 100	~50 (2)	65	75	[116]
ZnO-O Nanofibers				~125 (2)	75	125	
ZnO-H Nanofibers				~80 (2)	130	135	
ZnO Nanofibers	Electrospinning technique / Sol-gel method	200	H_2S / 1	~55% (3)	14	87	[104]
Cu-ZnO Nanofibers				83.98% (3)	9	160	
ZnO Nanosheets	Hydrothermal reaction	307	Ethanol / 200	212 (2)	8	7	[145]
Au-ZnO Nanosheets	Hydrothermal reaction	300	Ethanol / 60	35% (2)	15	-	[146]
ZnO Nanosheets	Hydrothermal reaction	RT	H_2 / 100	115% (4)	~9	6	[147]
GQD-SnO_2/ZnO	-	RT	H_2S / 0.1	15.9 (2)	14	13	[148]
Nanosheets							
Pd-ZnO Nanosheets	Solvothermal method	300	H_2 / 50	2.514 (2)	-	-	[149]
			Benzene / 50	1.241 (2)			
			Toluene / 50	1.312 (2)			
			CO / 50	1.208 (2)			
ZnO Nanoplates	Hydrothermal reaction	250	Formaldehyde	~2 (6)	80	60	[150]
			/ 1				
ZnO Nanosheets	Hydrothermal reaction	200	NO_2 / 1	2.0 (5)	~30	~400	[151]
ZnO Nanosphere				2.2 (5)	-	-	
ZnO Nanoplates				156 (5)	~30	~300	
Zn Nanoflowers	Hydrothermal reaction	RT	NO_2 / 1	128 (4)	360	240	[152]
Zn Nanoflowers	Hydrothermal reaction	250	NO_2 / 1	~25 (2)	-	-	[153]
Zn nanorods			C_6H_6 / 10	~3 (2)			
			EtOH / 20	~18 (2)			
			NO_2 / 1	~15 (2)			
			C_6H_6 / 10	0 (2)			
			EtOH / 20	~20 (2)			

ZnO-U – untreated/ ZnO-O - Oxygen-plasma-treated **ZnO-H - Hydrogen-plasma-treated**
(1) S = (Rair - Rgas)/ Rair x 100% (2) S = Rair/ Rgas
(3) S = (Rgas - Rair)/ Rair x 100% (4) S = (Rair - Rgas)/Rgas x 100%
(5) S = Rgas/Rair

temperature, they greatly increase the sensor response, due to the greater contact of the gas of interest with the sensor surface [134].

5. ZnO structures for chemiresistive gas sensing

As mentioned before, ZnO has been employed to design chemiresistors, in which changes of electrical resistance occurs when gas molecules react onto its surface [43]. Specifically, oxygen molecules adsorbed on the surface of the ZnO can ionize in oxygen species (O_2^-, O^-, O^{2-}) [135], capturing electrons from the conduction band, leading to formation of the depletion layer and, thus, increasing the resistance of the sensor [43]. When reducing gases, such as ethanol, approach the ZnO surface, oxygen species will interact with these gas molecules and release electrons trapped back into the conduction band, causing the resistance of the sensor to decrease [38,136,137]. During exposure to oxidizing gases as SO_2, which act as an electron acceptor, the resistance of the sensor increases [38,138]. In this way, gas detection is achieved by varying the resistance of the sensor [43]. Currently, efforts have been devoted to develop miniaturized chemiresistors using zero dimensional (0D), one dimensional (1D), two dimensional (2D) and three dimensional (3D) nanostructures. The Table 1 presents a compilation of some of the most relevant works reporting ZnO sensors based on different morphologies. Besides, a few of them were selected to be presented and discussed in more details in the next subsections.

5.1. ZnO nanoparticles and quantum dots

ZnO nanoparticles and quantum dots exhibit 0D morphology and high surface area-to-volume ratio, which is key to increase the sensor's figure of merit [154]. The techniques employed for developing nanoparticles and quantum dots (QDs) with controlled size and shape include spray pyrolysis [138], hydrothermal method [140,155,156], sol gel [139,157–159], wet chemical method [40,45,141] and others. It is very important to control the growth rate and the nucleation process to achieve nanoparticles and QDs with suitable properties for sensing applications, and usually chemical processes are the preferred over other methods. As an example, Niarchos et al. explored sol-gel method to

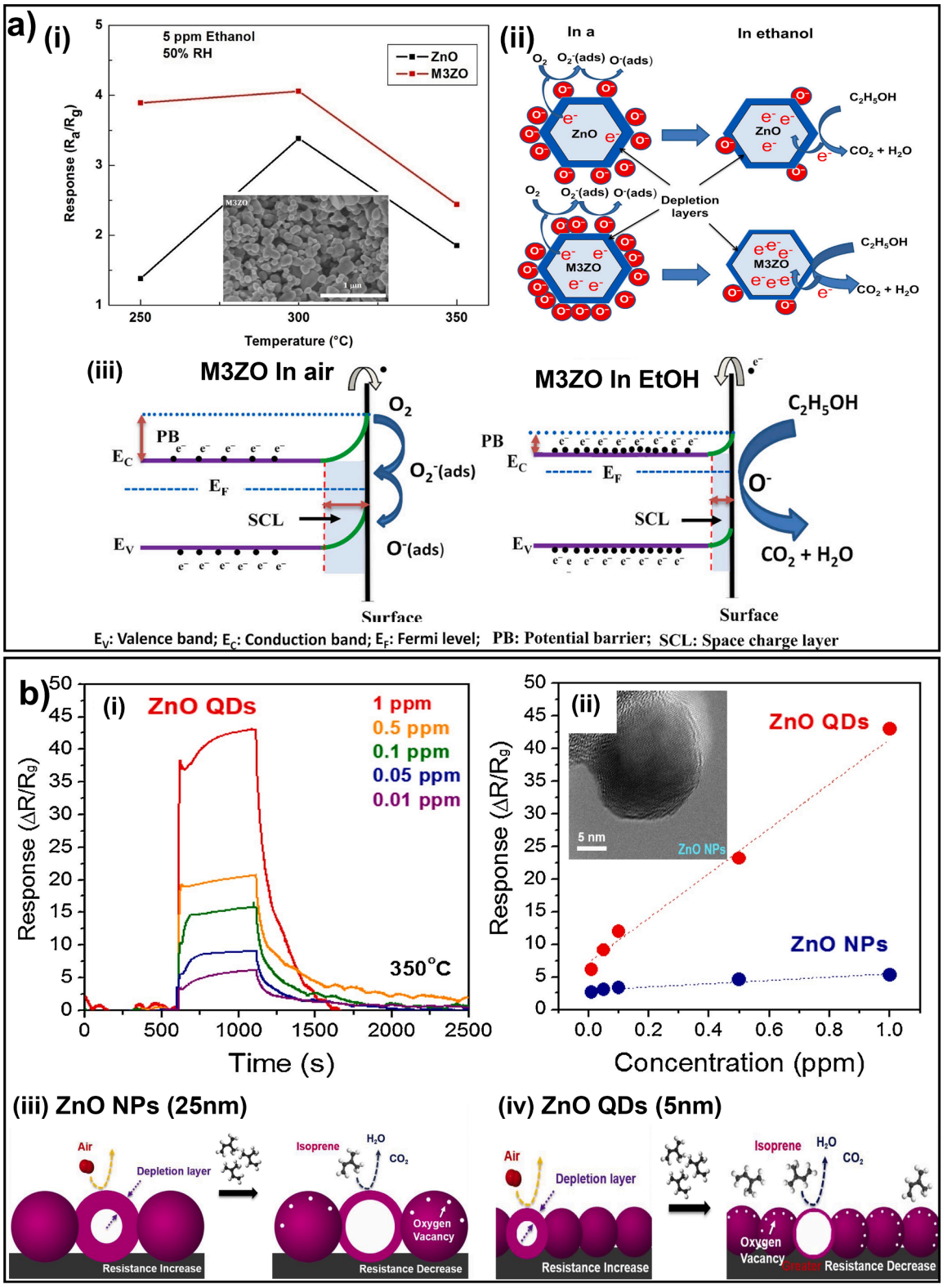

Fig. 6. (a) ZnO NPs doped with Mg (yielding the sample M3ZO) (i) Comparison of the sensing platforms in the presence of 5 ppm of ethanol, (ii) schematic representation of ethanol sensing mechanism and (iii) SEM images of M3ZO and (iv) energy band structure of M3ZO based on the proposed sensing mechanism. Reprinted with permission from Ref. [157]. (b) (i) dynamic response curves of ZnO QDs at 350 °C as a function of isoprene concentration, (ii) sensing response comparison for ZnO NPs (blue) and ZnO QDs (red) for isoprene concentration ranging from 0.01 to 1 ppm, the inset presents SEM images of ZnO QDs, schematic representation of the sensing mechanism for (iii) ZnO NPs and (iv) ZnO QDs. Reprinted with permission from Ref. [163].

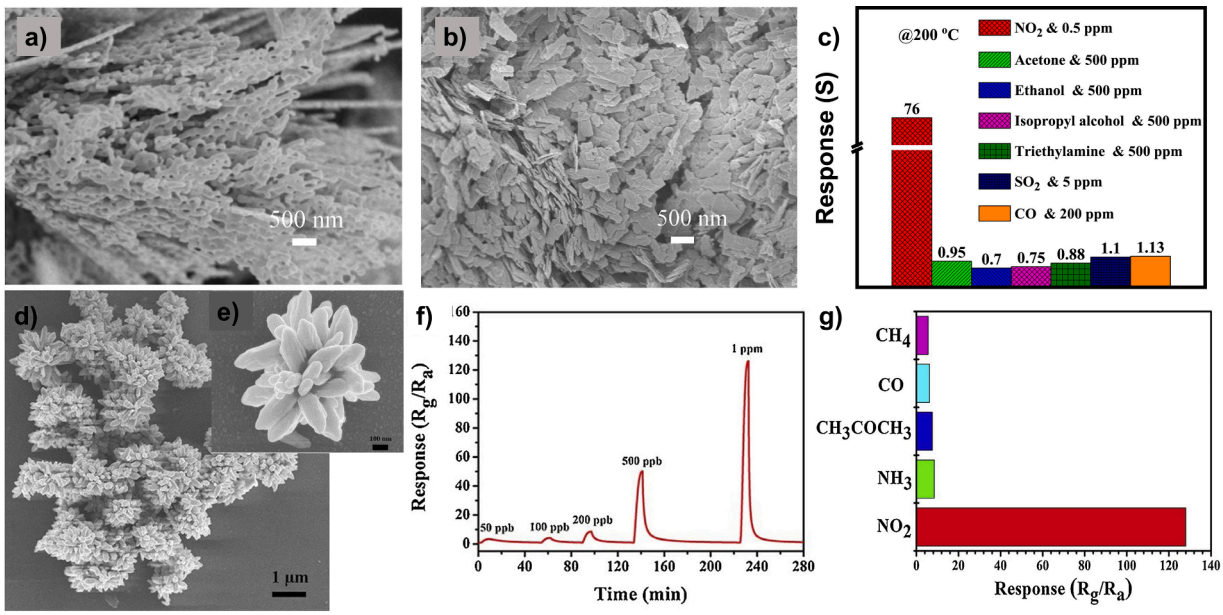

Fig. 7. Scanning electron microscopy of ZnO (a) nanosheets and (b) nanoplates. (c) Sensor response and selectivity towards 0.5 ppm of NO_2. Reprinted with permission from Ref. [151]. (d) Scanning electron microscopy of ZnO nanoflowers, (e) ZnO nanoflowers, (f) sensor response to low concentrations of NO_2 and (g) sensor selectivity towards 5 analytes. Reprinted with permission from Ref. [152].

synthetize ZnO nanoparticles further applied as humidity sensor by spreading the nanoparticles onto electrodes (paper) surface and annealing at 100°C to bind the material as a film. Nanoparticles coalescence resulted in better long-term stability proving to be an alternative material to improve paper-based devices stability over humidity [158].

ZnO nanoparticles morphology can be designed to improve sensitivity and selectivity, where the surface reactivity is dependent on the metal oxide crystalline faces facing out [37,68,160]. In this direction, Ryzhikov et al. [161] prepared ZnO nanoparticles (NP) with different morphologies (nanorods, isotropic, and cloud-like) by organometallic route and tested them as gas sensor for CO, C_3H_8, and NH_3. ZnO NP morphology showed significant influence on sensors response and selectivity for reducing gases. Nanorods showed the highest response to C_3H_8 and CO, whereas, for NH_3 detection no effect of morphology could be observed [161]. The authors highlighted that the ZnO nanoparticles control was made without drastic changes on the synthetic route and that the sensor response and selectivity could be related to basal and lateral crystalline faces presence and percentage, justifying the nanorod higher sensitivity to propane.

Another strategy highly explored to improve nanostructured ZnO performance as gas sensor is the doping process of ZnO. For instance, Jaballah et al. [157] prepared sensing devices based on ZnO NPs and ZnO NPs doped with Mg (Fig. 6a (i–iii)). The Mg-ZnO (M3ZO) platform showed a response 200% higher than pristine ZnO NPs for 5 ppm of ethanol at 250 °C, best operating temperature (Fig. 6a (i)). The proposed sensing mechanism explores the idea of ethanol acting as a reducing gas by interaction with oxygen species adsorbed at the oxide surface (Fig. 6a (ii)). Once the gas is adsorbed, oxygen species release the trapped electrons from the depletion layer to the oxide bulk decreasing its electrical resistance (Fig. 6a (iii)). The authors estimated that by doping ZnO with Mg^{2+}, the adsorption of oxygen species during the material synthesis is favored since the dopant will act as donor. Once the gas sensing is dependent on these oxygen species, higher concentration of oxygen species led to improved sensing response to ethanol [157].

Metal oxide quantum dots have also demonstrated promising sensing performance, indicating that very small particles (2–10 nm) with charge carriers confined in all three spatial dimensions can boost electrical properties of semiconductors, offering insights to the new era of gas sensors [154,162]. Specifically, ZnO QDs have also been successfully applied in chemiresistive sensors, being one of the three most explored metal oxide quantum dots along with SnO_2 and TiO_2 [154]. In this direction, ZnO QDs with different grain sizes can be obtained by wet chemical method with different reaction times as a parameter able to modulate sensors response to gas analytes such as demonstrated by Hu et al [141]. In this case, the sensors demonstrated direct correlation between signal response and crystal grain size when applied to H_2S sensing. This correlation could be corroborated by mathematical calculation method [141]. Comparing ZnO QDs with ZnO NPs it is possible to observe the better performance of ZnO QDs (Fig 6b(i, ii)) [163]. Both ZnO NPs and ZnO QDs sensing is based on the same mechanism, the depletion theory. Nevertheless, ZnO QDs presents higher resistance once the band gap is larger thanks to quantum confinement effect and higher amount of oxygen vacancies (Fig. 6b (iii, iv)). Therefore, ZnO QDs and their greater number of surface-sensing active sites for isoprene adsorption leads to increased sensing response.

In another example, researcher synthesized ZnO QDs with ~2.53 nm of diameter and showed a high selective response towards H_2 when compared to the other six (interferents) volatiles [45]. In this case, ZnO QDs sensitivity and selectivity could be addressed to the reaction of H_2 molecules with oxygen species adsorbed onto the sensor surface, and then with ZnO creating acceptor surface states and releasing electrons to ZnO QDs bulk. Moreover, QDs have been largely exploited in combination with other compounds as sensing layer. In a recent study, Sun et al prepared a mixed platform using ZnO QDs and SnO_2 hollow nanospheres, which hybrid platform showed a better sensing performance towards formaldehyde than the sensors based on the pristine of ZnO QDs and pristine SnO_2. The improvement was attributed by the authors as a heterojunction formation resulting from the distinct materials combination [40]. More examples of hybrid material obtained with ZnO QDs are discussed in further sections.

5.2. 1D ZnO nanostructures

One-dimensional ZnO nanostructures are versatile materials employed in supercapacitors [164], photocatalytic degradation [165] and batteries [166]. Additionally, these structures have also been applied in gas sensors [167] in varied morphologies, such as nanotubes

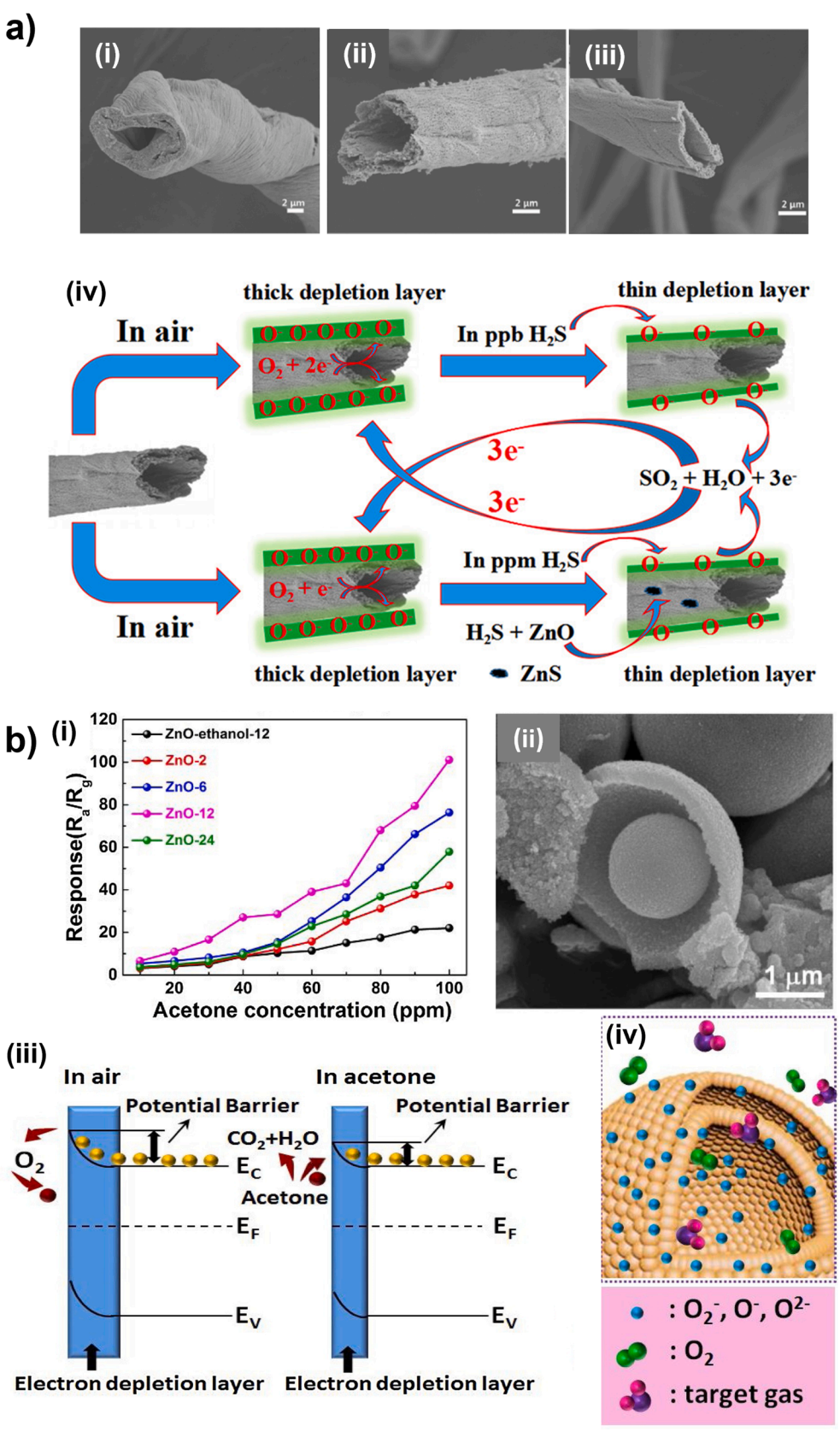

Fig. 8. (a) SEM images of hollow ZnO nanotubes obtained at (i) 500 °C, (ii) 600 °C and (iii) 700 °C, (iv) schematic representation of proposed sensing mechanism for hollow ZnO nanotubes obtained at 600 °C. Reprinted with permission from Ref. [198]. (b) (i) sensing response of single-shelled ZnO (ZnO-2), double-shelled ZnO (ZnO-6), double shelled ZnO (ZnO-12), singles shelled ZnO (ZnO-24) and ZnO microparticles (ZnOethanol-12) at 300°C upon exposure to acetone, (ii) SEM image of ZnO hollow microspheres, (iii) schematic representation of proposed depletion layer and (iv) ZnO hollow microspheres sensing mechanism. Reprinted with permission from Ref. [199].

Table 2
Overview of room temperature sensors employing composites based on ZnO.

Materials	Operating temperature /°C	Gas and concentration / ppm	Response (S)	Response time / s	Recovery time / s	Ref.
ZnO nanosheets – Aniline	RT	NH_3 / 10	2150% (1)	431 (for 5 ppm)	387 (for 5 ppm)	[160]
ZnO	130	Methanol / 100	7 (2)	~17.5	~15	[202]
ZnO-PANI	60		19.2 (2)	18.2	5.1	
PPY	26	NH_3 / 50	24 (3)	-	-	[203]
ZnO nanorods – PPy			41 (3)	23	62	
ZnO nanorods – PPy – CSA			77 (3)	21	51	
ZnO nanoparticle	200	NO_2 / 100	14 (4)	-	-	[204]
ZnO nanoparticle – PPy	RT		37 (4)	120-240	24h	
ZnO Nanofibers	RT	NH_3 / 100	~2 (4)	-	-	[205]
ZnO Nanofibers – PPS			~10 (4)	51	160	
ZnO@CuO	RT	H_2S / 10	20,7 (5)	33	298	[206]
ZnO@Ag	RT	Ethylene /	4.05 (4)	300	600	[207]
		30	4.48 (4)	435	1430	
		50				
ZnO@SiO_2/rGO	29	Ethanol / 300	131.7 (5)	-	-	[46]
		Methanol / 300	21.8 (5)			
		1-propanol / 300	156.85 (5)			
ZnO NS	RT	Aniline / 100	1.5 (5)	-	-	[208]
ZnO@CeO			15.1 (5)	67	113	
ZnO/Au	RT	NH_3 / 10	~15% (0%RH) (6)	4440 (0%RH)	1680 (0%RH)	[209]
			~13% (20%RH) (6)	1200 (20%RH)	180 (20%RH)	
ZnO/graphene	RT	NO_2 / 5	6.78% (1)	193	2022	[210]
ZnO/GO	RT	NH_3 / 50	~60 (5)	19	73	[211]
GO			~2.1 (5)	250	240	
ZnO	RT	NH_3 / 1000	~200 (5)	-	-	[212]
ZnO:GQDs			6047 (5)			
ZnO:rGO	RT	NO_2 / 1.5	1.4 (2)	405	760	[213]
		H_2S / 20	2.68 (2)	404	275	
Graphene/ZnO nanorods	RT	CO / 10-90	21.68-41.08 (4)	435-370	45-115	[214]
(1) $S = (R_g\text{-}R_a)/R_a$ x 100		(2) $S = (R_a\text{-}R_g)/R_g$ x 100				
(3) $S = (R_g\text{-}R_a)/R_g$ x 100		(4) $S = (R_a\text{-}R_g)/R_a$ x 100				
(5) $S = R_a/R_g$		(6) $S = (I_g - I_a)/I_a$ x 100				

[168,169], nanowires [142,170–172], nanoneedles [143,144, 173–175], and nanofibers [104,176–179].

The judicious choice of the production method and associated parameters can be an excellent way to improve the material performance towards sensing applications [142]. For example, when ZnO nanowires are prepared by electrospinning and calcined at different temperatures, the resulting material might present different performance over gas detection based on the junction formation for each treatment temperature. The temperature optimization can be an ally on the sensing performance improvement [142], as well as the optimization of all synthesis parameters might direct influence the sensor performance. Post treatment of ZnO nanostructures is also a strategy for properties modulation and improvement of sensing properties. Researchers have explored low-temperature plasma treatment of electrospun ZnO nanofibers aiming to increase nanofibers surface area and porosity for better gas sensing performance [116]. This proposition could be corroborated by DTF calculations and adsorption energy variation according with ZnO nanofibers surface treatment. Such evidence indicates the direct influence of plasma treatment on electrons movement and electrical resistance after exposure to the gas analyte. Thus, the improvement of 1D sensor properties of ZnO has been increasingly expanded beyond the conventionally found structures. Aside from the high surface area and great amount of available active sites, ZnO 1D nanostructures sensing mechanism is benefited from improved charge carriers' mobility thanks to a continuous conducting channel formed along the 1D preferential axes. With that in mind, it would be very welcome future contributions comparing the length of 1D nanostructures based on the same material with its sensing performance. Besides solid and porous ZnO 1D nanostructures, hollow ZnO nanofibers have also been extensively explored in gas sensors and although it is a 1D morphology, the most recent classification indicates its 3D character, evidenced by the internal exposed surface available for gas adsorption. For that reason, hollow ZnO nanofibers will be discussed along with nanoflowers and hollow spheres in Section 5.4.

5.3. 2D ZnO nanostructures

The development of 2D materials composed of a single or a few atomic layers has been shown to be a promising strategy for optoelectronic devices. Graphene, for example is a 2D material that has aroused enormous scientific interest owing to their appealing mechanical, electrical and optical properties [145] combined to high porous volume for gas diffusion [180]. All these features have driven the development of sensor devices that show high sensitivity to toxic gases with fast response. Two common ZnO 2D nanostructures normally employed as sensors are nanosheets [147–149,151,181] and nanoplates [182,183]. In order to compare different 2D morphologies in sensors application, Duy et al. prepared platforms based on ZnO nanosheets (Fig. 7a) and nanoplates (Fig. 7b) exposed to low concentrations of NO_2. By modulating the hydrothermal synthesis parameters, materials with different morphologies and related sensing behaviors could be achieved. The nanoplates were characterized to have a 15 nm thickness, which is almost 10 times smaller than 3D ZnO (~100 nm). Besides lower thickness, 2D ZnO is also highlighted by the increased surface area and both together contribute for a high response ($S = 76$ for 0.5 ppm of NO_2) and selectivity towards NO_2 against acetone, ethanol, isopropyl alcohol, triethylamine, SO_2 and CO (Fig. 7c) [151]. Furthermore, the authors reported a calculated limit of detection of 3 ppt towards NO_2.

5.4. 3D ZnO nanostructures

3D ZnO nanostructures are advanced morphologies that can be employed for developing chemiresistive sensors with interesting properties [184–186], although some limitations may occur owing to the difficult to control the synthesis parameters and limited production rate [187]. ZnO nanoflowers, for instance, have been successfully employed in chemiresistive sensors by distinct research groups through different methods [153,188–192]. Song et al. have prepared ZnO nanoflowers (Fig. 7d, e) by a hydrothermal method with average diameter of 0.9–1

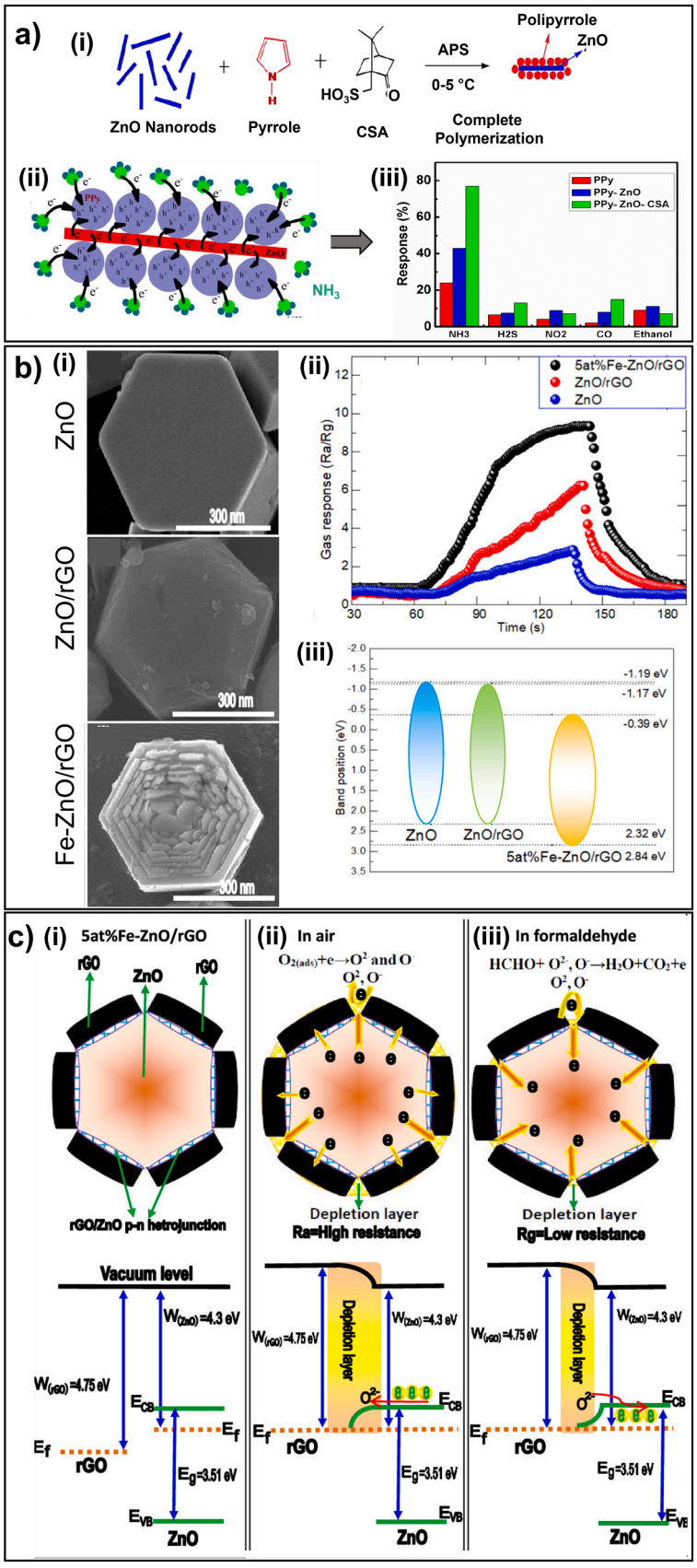

Fig. 9. (a) (i) *In-situ* oxidative polymerization of polypyrrole-ZnO-CSA nanocomposite, (ii) Ammonia gas molecules adsorption and (iii) electrical response of polypyrrole-ZnO-CSA nanocomposite towards ammonia, H_2S, NO_2, CO and ethanol. Reprinted with permission from reference [203]. (b) (i) Scanning electron microscopy of ZnO, ZnO/rGO and 5 atom% Fe-ZnO/rGO, (ii) sensor response of ZnO, ZnO/rGO, and 5 atom% Fe−ZnO/rGO to 5 ppm of formaldehyde, (iii) structure of energy band for ZnO, ZnO/rGO, and 5 atom% Fe−ZnO/rGO, (c) (i-iii) schematic illustration of the proposed sensing mechanism for Fe−ZnO/rGO nanocomposites. Reprinted with permission from Ref. [223].

μm without any doping or modification. The pure ZnO nanoflowers sensing performance towards NO_2 monitoring (Fig. 7f) was attributed to the formation of an Schottky barrier between the ZnO film and Au electrodes yielding to a detection limit of 50 ppb and high selectivity for NO_2 (Fig. 7g) [152].

3D ZnO nanostructures are usually composed by hollow spheres and nanofibers. Usually, multiple steps reactions and methods are necessary to achieve hollow nanostructures which is time consuming and costly [32]. Therefore, the development of straightforward and effective one-step synthetic rout to produce hollow nanostructures is still challenging. Both hollow ZnO nanofibers/nanotubes/nanoneedles and spheres have been explored for gas sensing and their properties studied to better understand its influence on the final sensing performance. Some reports defend the electron-hole pair segregation, where electrons are located on the external surface while the majority of holes are located on the internal surface [193–195]. Sensor response time has been related to wall thickness of hollow ZnO nanotubes, indicating that response time can be greatly decreased by reducing the wall thickness [196]. Besides, sensor response can be improved by enhancing the number of shell structures in hollow ZnO nanospheres [197]. Moreover, hollow ZnO nanostructures are advancing on the pathway of large-scale production as demonstrated by Na et al. [198]. The authors achieved hollow ZnO nanotubes as sensor device for H_2S detection with outstanding figures of merit such as surface area of 31 m^2g^{-1}, response time of 29 s and sensor response of 85% for 10 ppm of H_2S for optimized synthesis temperature (Fig. 8a (i–v)). For hollow ZnO structures, it has been demonstrated that double-shelled can operate on gas sensing detection with a response time of 1 second upon exposure to 100 ppm of acetone along with low limit of detection, low temperature of operation and high selectivity (Fig. 8b (i, ii)) [199]. The sensing mechanism for hollow spheres consider the depletion theory in which oxygen species are adsorbed onto double-shelled ZnO hollow microsphere surfaces capturing electrons from ZnO conduction band and releasing them when in contact with the target gas (Fig. 8b (iii)). Besides, the interspace between the shells is advantageous to gas diffusion as well as double shells offering large active sites ensuring the gas access from different direction and resulting in high response (Fig. 8b (iv)).

6. ZnO heterostructures for chemiresistive gas sensing

As discussed in the previous sections, sensors based on semiconductor oxides in general require high temperature to control their kinetics, electron mobility and activation of reactive sites [200]. Other drawbacks are the energy costs associated with heating the device and the high temperatures can trigger explosions with flammable gases and create measurement instability [74,200] in addition to induce crystal growth and loss of sensitivity. In this way, different approaches have been explored to develop sensors that can operate at room temperature with long-term stability [74,200,201]. The additive doping has been extremely explored for this propose where four classes of materials can be highlighted: metals, inorganic materials, conducting polymers and carbon materials. A collection of some of the most relevant works reporting ZnO/nanocomposites sensors for operation at room temperature are summarized in Table 2. Besides the compilation of these results in Table 2, a few of them were selected to be presented and discussed in the next subsections. Next, we present the major classes of materials that have been explored for the development of ZnO-based nanocomposites.

6.1. Conductive polymer composites

Composites using conductive polymers have attracted great attention mainly due to their ease of production and interesting optical and electrical properties [215]. These materials can be explored in areas as catalysis [216], batteries [217], supercapacitors [218] and sensors [219–221]. However, it is worth mentioning that sensing platforms based on some polymers can respond to multiple gases at room temperature and undergoing quick degradation. In this way, the association of this material with SMOs has overcome different limitations presented by their separate phases such as high working temperatures (oxides) and low selectivity (polymers) [222]. A wide variety of works have demonstrated ZnO-based composites with high sensitivity and stability at room temperature [160,202–205].

ZnO nanostructures have been combined with polyaniline (PANI), polypyrrole (PPY), poly(3,4-ethylenedioxythiophene) (PEDOT) among others for sensing and detection applications. For instance, ZnO combined with PANI as a hybrid platform presented sensor response to 100 ppm of methanol 2.5 higher than the pure ZnO platform [202]. Besides, the combination of ZnO with PANI can result in operating temperature optimization by improving metal oxide performance at mild temperatures. Such behavior can be attributed to the formation of a heterojunction between the ZnO and the conjugated polymer [202]. The heterojunction formation will further contribute to improved sensor response once the depletion layer formed at the junction presents a lower energy barrier, thus favoring the charge transfer. The response of ZnO/conjugated polymers platforms can be even further optimized using a complex doping process. For example, Jain et al. studied the performance of three different platforms using PPy (polypirol), PPy-ZnO, PPy-ZnO-CSA (camphor sulphonic acid) produced by *in-situ* polymerization (Fig. 9a, b). The complex platform (PPy-ZnO-CSA) showed the better performance towards ammonia detection (Fig. 9c), with a response of ~80% contrasting with a response of ~40% with the PPy-ZnO plataform, due to the electronic delocalization created by the CSA, which has increased the interaction with the analyte and the selectivity to ammonia against H_2S, NO, CO and ethanol [203].

6.2. Carbon materials adding

Carbon materials as doping elements have been employed in the design of chemiresistive sensors. Common examples that can be site are carbon nanotubes [224,225], graphene [210,226], carbon black [227,228], carbon nanofibers [229]. These materials are known for their good stability, electrical conductivity, and for the surface defect sites which can be created when employed in nanocomposites with other materials [229]. Their utilization with metal oxides have proved to be very promising to develop sensing platforms highly sensitive at room temperature [212,214]. In this way, further improvements have been made to combine different carbon materials in functional sensing platforms for operating at room temperature with high sensing performance. Guo et al. reported a tertiary nanocomposite in which reduced graphene oxide was combined with ZnO and doped with Fe (Fig. 9d). The nanocomposite was explored towards formaldehyde sensing and showed improved response when compared with pristine ZnO and ZnO/rGO as shown in Fig. 9e. This composition allowed the sensor to operate in lower temperature than common formaldehyde sensors reaching the detection of a minimum concentration of 5 ppm at this temperature. The valence band level could be determined by VB XPS (Fig. 9f) and showed a shift of Fe−ZnO/rGO CB level as a result of Fe doping and rGO intimate interaction with ZnO. This Fe−ZnO/rGO CB level shift was responsible for generating more electrons, increasing the content of adsorbed oxygen species and ultimately improving the sensing performance (Fig. 9g–i) [223].

Besides electrical properties improvements, carbon-based materials such as graphene can contribute to the design of flexible and wearable ZnO sensors. For instance, Utari et al. have developed flexible platforms based on graphene/ZnO nanocomposite highly sensitive and selective towards CO. The graphene/ZnO nanocomposite showed a 40% higher sensitivity than bare graphene. By combining p-type graphene with n-type ZnO, the Fermi levels will be aligned causing a band bending as the electrons are transferred from ZnO to graphene. The potential barrier formed at the interface will receive electrons from CO gas during exposure giving the resistance change as sensor response [214]. The same behavior was observed by Wongrat et al., who developed ZnO

nanostructures decorated with graphene QDs reported a superior electrical response towards NH_3 at room temperature compared to the platform based only on ZnO. The QDs provides carboxyl and hydroxyl groups to the system enabling a higher amount of water absorption trough hydrogen bonds. Such behavior increases the content of H^+ leading to a response 2 order of magnitude higher and great selectivity (more than 30 times higher response) towards ammonia against ethanol and acetone [212]. Additionally to the works presented in this topic, the addition of carbon materials to ZnO composites can be seen as one way to create surface defect sites and increase the adsorption of target gases on those platforms, consequently increasing the sensor response.

6.3. Metal and inorganic adding

A large range of metals such as Pt [181,183], Ag [143,159], Pd [149, 182,230], Al [231], Mg [157], Cu [232], Au [39,146,193,233], Cr [139, 234] and Mn [235] have been employed in combination to ZnO to produce hybrid sensing platforms. It is worth noting that the addition of metals can result in different behaviors for each platform: in some cases, the improvement in some parameters (device response and working temperature) is observed, while in other cases only one parameter is changed. This behavior can be explained by the nature of the added metal where two effects can be observed: chemical effects and electrical effects [236].

The chemical effect concerns the increase in the adsorption rate of oxygen molecules (O_2) and their dissociation into atomic species (O) on the material surface. This process is responsible for generating an electron flux from the conduction band of ZnO that will be used for the ionization of these atomic species. This phenomenon will stimulate the creation of a depletion layer in the material, which in turn will change its electronic structure and improve the electrical performance [73]. However, the opposite phenomenon can be also observed. In this case, the electrical effect created by the work function difference between the oxide and metallic material can influence electron extraction from the oxide structure and also create a depletion barrier which will obstruct the electronic movement and consequently decrease the sensor performance at room temperature [38]. In this way, the addition of metals can show some drawbacks, so it is very important the judicious choice of materials. For example, Kim et al. reported a sensor employing a hybrid structure of Au@ZnO nanowires towards CO. The authors found higher performance and lower operating temperature to the hybrid platform compared to the ZnO pure platform. The sensor based only on the nanowires showed good response at 300°C while the hybrid platform showed high sensitivity at room temperature [47]. In this case, it can be observed that the doping process was successfully used to create better response at room temperature. However, the same behavior is not always observed. Nagarjuna and Hsiao have developed sensing platforms for ethanol employing Au as a doping element for ZnO nanosheets. The authors noted an increase of 75% in the sensor response for 60 ppm of ethanol between the hybrid platform and the platform based only in ZnO nanosheets. However, the optimum working temperature of the platforms remained at 300 °C [146], suggesting that the doping process is not always associated with room temperature sensors.

Similarly to metals, inorganic oxides have also been explored as doping agents in sensors [206–208]. In this direction, Zhang et al have prepared sensing platforms using Ce as a doping material to ZnO nanosheets. The authors observed an improvement in sensor performance for the hybrid platforms attributed to an increase in oxygen vacancies, higher surface area and intimate interface interaction between the materials. The good properties obtained with the hybrid 2D structure were explained based on a proposed sensing mechanism that consider the oxygen vacancies content increased by Ce doping, which in turns increase the content of oxygen species adsorbed on the metal oxide surface working as adsorption sites for the target gas [208]. Even more complex combinations have been proposed aiming to boost the sensor performance. For example, Samadi et al. have proposed a sensing

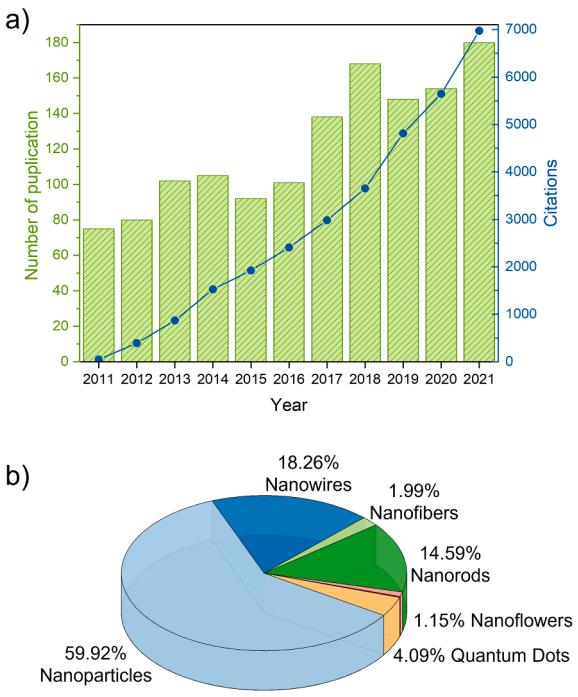

Fig. 10. (a) Number of scientific publications and patents (green histogram) and citations (blue circles) per year (from 2011 to 2021) related to zinc oxide for chemiresistive gas sensors applications. (b) Distribution of published articles according to the ZnO morphology. Data obtained from Web of Science accessed in March 2022 using the keywords "zinc oxide'' and "gas sensor'' and "chemiresistive sensor".

platform using ZnO@SiO_2/rGO core/shell composite towards 1-propanol at room temperature. The reduced graphene add to the ZnO@SiO_2 structure turns to be responsible for the improved response once it contributes to an increase of electrical current by the heterojunction formation at the interface of the hybrid structure created with ZnO@SiO_2 when exposed to the target gas [46]. The overall response is higher than with ZnO@SiO_2 once the initial state of ZnO@SiO_2/rGO is more resistive and the final state, after exposure to the gas, is more conductive than ZnO@SiO_2 resulting in improved sensing response.

7. Conclusions and perspectives

In this review, we surveyed recent developments in ZnO-based chemiresistive gas sensors over the last decade. ZnO has captured a great deal of interest thanks to its excellent properties for sensing varied analytes as alcohols, ethers, ammonia, (NO)x, H_2S, SO_2 and CO. The development and improvement of synthesis techniques have enabled the synthesis of hierarchical and functional ZnO structures, which have been widely explored for sensing applications, as discussed throughout this review. A great emphasizes has been given on the production of ZnO-based (organic and hybrid) composites with controlled morphology, shape and surface to enhance sensing performance regarding sensitivity, selectivity, response and recovery time as well as long-term stability. Specifically, it has been demonstrated that dissimilar materials in nanocomposites can yield suitable heterojunctions or ion-doped structures presenting structural characteristics that favor the charge carrier mobility and transfer, enabling amplified sensing signal when exposed to the target analyte. Moreover, it is important to emphasize that both materials choice and morphologies (being this latter aspect highly influenced by the synthesis method and parameters employed) are key in the final sensing performance. The ongoing relevance of chemiresistive ZnO based sensors can be visualized in Fig. 10a by the number of publications/citations in the literature over the past decade, indicating

the field still have room for studies and exploration. In terms of ZnO morphology, one observes that nanoparticles are the most popular choice probably due to the ease and well-known syntheses methods (Fig. 10b). Followed by nanowires and nanorods are the top three morphologies most common for ZnO applied in chemiresistive sensors. Another interesting data from this analysis is the fact that ZnO nanofibers represents only 2% of total reports indicating an alternative for further exploration when it comes to ZnO chemiresistive gas sensors.

Nevertheless, some challenges still need to be overcome regarding the influence of humidity in the sensing response and precise control on the composite's morphology, especially when using 3D nanomaterials. Besides, flexible, portable, and transparent chemiresistive sensors based on nanostructured ZnO can also be considered a potential approach for wearable sensor devices.

Declaration of Competing Interest

The authors declare no conflict of interest.

Acknowledgements

The authors thank the financial support from FAPESP (Grant Nos.: 2016/23793-4, 2017/12174-4, and 2018/22214-6), CNPq, MCTI-SisNano (CNPq/402.287/2013-4), CAPES (Grant No.: 001) and Rede Agronano (EMBRAPA) from Brazil.

References

[1] Z. Li, J.R. Askim, K.S. Suslick, The optoelectronic nose: colorimetric and fluorometric sensor arrays, Chem. Rev. (2018), https://doi.org/10.1021/acs.chemrev.8b00226.
[2] T.R. Pavase, H. Lin, Q. Shaikh, S. Hussain, Z. Li, I. Ahmed, L. Lv, L. Sun, S.B. H. Shah, M.T. Kalhoro, Recent advances of conjugated polymer (CP) nanocomposite-based chemical sensors and their applications in food spoilage detection: A comprehensive review, Sensors Actuators B Chem. 273 (2018) 1113–1138, https://doi.org/10.1016/j.snb.2018.06.118.
[3] N.R. Tanguy, M. Thompson, N. Yan, A review on advances in application of polyaniline for ammonia detection, Sens. Actuators B Chem. 257 (2018) 1044–1064, https://doi.org/10.1016/j.snb.2017.11.008.
[4] X. Yan, H. Li, X. Su, Review of optical sensors for pesticides, TrAC Trends Anal. Chem. 103 (2018) 1–20, https://doi.org/10.1016/j.trac.2018.03.004.
[5] C. Di Natale, R. Paolesse, E. Martinelli, R. Capuano, Solid-state gas sensors for breath analysis: a review, Anal. Chim. Acta 824 (2014) 1–17, https://doi.org/10.1016/j.aca.2014.03.014.
[6] H. Nazemi, A. Joseph, J. Park, A. Emadi, Advanced micro- and nano-gas sensor technology: a review, Sensors 19 (2019) 1285, https://doi.org/10.3390/s19061285.
[7] R.S. Andre, R.C. Sanfelice, A. Pavinatto, L.H.C. Mattoso, D.S. Correa, Hybrid nanomaterials designed for volatile organic compounds sensors: a review, Mater. Des. 156 (2018) 154–166, https://doi.org/10.1016/j.matdes.2018.06.041.
[8] G. Neri, First fifty years of chemoresistive gas sensors, Chemosensors 3 (2015) 1–20, https://doi.org/10.3390/chemosensors3010001.
[9] J.M. Rheaume, A.P. Pisano, A review of recent progress in sensing of gas concentration by impedance change, Ionics (2011), https://doi.org/10.1007/s11581-010-0515-1 (Kiel).
[10] F.G. Bănică, Chemical Sensors and Biosensors, John Wiley & Sons, Ltd, Chichester, UK, 2012, https://doi.org/10.1002/9781118354162.
[11] H. Wohltjen, W.R. Barger, A.W. Snow, N.L. Jarvis, A vapor-sensitive chemiresistor fabricated with planar microelectrodes and a Langmuir-Blodgett organic semiconductor film, IEEE Trans. Electron. Devices 32 (1985) 1170–1174, https://doi.org/10.1109/T-ED.1985.22095.
[12] T. Lin, X. Lv, Z. Hu, A. Xu, C. Feng, Semiconductor metal oxides as chemoresistive sensors for detecting volatile organic compounds, Sensors 19 (2019) 233, https://doi.org/10.3390/s19020233.
[13] Y. Wang, A. Liu, Y. Han, T. Li, Sensors based on conductive polymers and their composites: a review, Polym. Int. 69 (2020) 7–17, https://doi.org/10.1002/pi.5907.
[14] R.A. Potyrailo, Toward high value sensing: monolayer-protected metal nanoparticles in multivariable gas and vapor sensors, Chem. Soc. Rev. 46 (2017) 5311–5346, https://doi.org/10.1039/C7CS00007C.
[15] U.T. Nakate, P. Patil, B. Ghule, Y.T. Nakate, S. Ekar, R.C. Ambare, R.S. Mane, Room temperature LPG sensing properties using spray pyrolysis deposited nanocrystalline CdO thin films, Surf. Interfaces 17 (2019), 100339, https://doi.org/10.1016/j.surfin.2019.100339.
[16] J.K. Rajput, T.K. Pathak, V. Kumar, L.P. Purohit, Influence of sol concentration on CdO nanostructure with gas sensing application, Appl. Surf. Sci. 409 (2017) 8–16, https://doi.org/10.1016/j.apsusc.2017.03.019.
[17] J. Ma, H. Fan, W. Zhang, J. Sui, C. Wang, M. Zhang, N. Zhao, A. Kumar Yadav, W. Wang, W. Dong, S. Wang, High sensitivity and ultra-low detection limit of chlorine gas sensor based on In2O3 nanosheets by a simple template method, Sens. Actuators B Chem. 305 (2020), 127456, https://doi.org/10.1016/j.snb.2019.127456.
[18] C.S. Lee, H.Y. Li, B.Y. Kim, Y.M. Jo, H.G. Byun, I.S. Hwang, F. Abdel-Hady, A. A. Wazzan, J.H. Lee, Discriminative detection of indoor volatile organic compounds using a sensor array based on pure and Fe-doped $In2O_3$ nanofibers, Sens. Actuators B Chem. 285 (2019) 193–200, https://doi.org/10.1016/j.snb.2019.01.044.
[19] X. Wang, T. Wang, G. Si, Y. Li, S. Zhang, X. Deng, X. Xu, Oxygen vacancy defects engineering on Ce-doped α-Fe_2O_3 gas sensor for reducing gases, Sens. Actuators B Chem. 302 (2020), 127165, https://doi.org/10.1016/j.snb.2019.127165.
[20] K. Tian, X.X. Wang, Z.Y. Yu, H.Y. Li, X. Guo, Hierarchical and hollow Fe_2O_3 nanoboxes derived from metal–organic frameworks with excellent sensitivity to H_2S, ACS Appl. Mater. Interfaces 9 (2017) 29669–29676, https://doi.org/10.1021/acsami.7b07069.
[21] C. Kamble, M. Panse, A. Nimbalkar, Ag decorated WO_3 sensor for the detection of sub-ppm level NO_2 concentration in air, Mater. Sci. Semicond. Process. 103 (2019), 104613, https://doi.org/10.1016/j.mssp.2019.104613.
[22] S. Büyükköse, Highly selective and sensitive WO_3 nanoflakes based ammonia sensor, Mater. Sci. Semicond. Process. 110 (2020), 104969, https://doi.org/10.1016/j.mssp.2020.104969.
[23] P.G. Choi, N. Izu, N. Shirahata, Y. Masuda, Improvement of sensing properties for SnO2 gas sensor by tuning of exposed crystal face, Sens. Actuators B Chem. 296 (2019), 126655, https://doi.org/10.1016/j.snb.2019.126655.
[24] M. Tonezzer, Selective gas sensor based on one single SnO_2 nanowire, Sens. Actuators B Chem. 288 (2019) 53–59, https://doi.org/10.1016/j.snb.2019.02.096.
[25] Y. Zou, S. Chen, J. Sun, J. Liu, Y. Che, X. Liu, J. Zhang, D. Yang, Highly efficient gas sensor using a hollow SnO_2 microfiber for triethylamine detection, ACS Sens. 2 (2017) 897–902, https://doi.org/10.1021/acssensors.7b00276.
[26] U.T. Nakate, G.H. Lee, R. Ahmad, P. Patil, Y.B. Hahn, Y.T. Yu, E. Suh, Nano-bitter gourd like structured CuO for enhanced hydrogen gas sensor application, Int. J. Hydrog. Energy 43 (2018) 22705–22714, https://doi.org/10.1016/j.ijhydene.2018.09.162.
[27] A. Umar, A.A. Ibrahim, U.T. Nakate, H. Albargi, M.A. Alsaiari, F. Ahmed, F. A. Alharthi, A.A. Alghamdi, N. Al-Zaqri, Fabrication and characterization of CuO nanoplates based sensor device for ethanol gas sensing application, Chem. Phys. Lett. 763 (2021), 138204, https://doi.org/10.1016/j.cplett.2020.138204.
[28] J.H. Bang, M.S. Choi, A. Mirzaei, S. Han, H.Y. Lee, S.W. Choi, S.S. Kim, H.W. Kim, Hybridization of silicon nanowires with TeO_2 branch structures and Pt nanoparticles for highly sensitive and selective toluene sensing, Appl. Surf. Sci. 525 (2020), 146620, https://doi.org/10.1016/j.apsusc.2020.146620.
[29] A.A. Mane, A.V. Moholkar, Orthorhombic MoO_3 nanobelts based NO_2 gas sensor, Appl. Surf. Sci. 405 (2017) 427–440, https://doi.org/10.1016/j.apsusc.2017.02.055.
[30] W. Jiang, L. Meng, S. Zhang, X. Chuai, Z. Zhou, C. Hu, P. Sun, F. Liu, X. Yan, G. Lu, Design of highly sensitive and selective xylene gas sensor based on Ni-doped MoO_3 nano-pompon, Sens. Actuators B Chem. 299 (2019), 126888, https://doi.org/10.1016/j.snb.2019.126888.
[31] J.W. Kim, Y. Porte, K.Y. Ko, H. Kim, J.M. Myoung, Micropatternable double-faced ZnO nanoflowers for flexible gas sensor, ACS Appl. Mater. Interfaces 9 (2017) 32876–32886, https://doi.org/10.1021/acsami.7b09251.
[32] J. Chao, Y. Chen, S. Xing, D. Zhang, W. Shen, Facile fabrication of ZnO/C nanoporous fibers and ZnO hollow spheres for high performance gas sensor, Sens. Actuators B Chem. 298 (2019), 126927, https://doi.org/10.1016/j.snb.2019.126927.
[33] S. Zhao, Y. Shen, X. Yan, P. Zhou, Y. Yin, R. Lu, C. Han, B. Cui, D. Wei, Complex-surfactant-assisted hydrothermal synthesis of one-dimensional ZnO nanorods for high-performance ethanol gas sensor, Sens. Actuators B Chem. 286 (2019) 501–511, https://doi.org/10.1016/j.snb.2019.01.127.
[34] Z.L. Wang, Nanostructures of zinc oxide, Mater. Today 7 (2004) 26–33, https://doi.org/10.1016/S1369-7021(04)00286-X.
[35] J. Xuan, G. Zhao, M. Sun, F. Jia, X. Wang, T. Zhou, G. Yin, B. Liu, Low-temperature operating ZnO-based NO_2 sensors: a review, RSC Adv. 10 (2020) 39786–39807, https://doi.org/10.1039/D0RA07328H.
[36] S. Chaudhary, A. Umar, K. Bhasin, S. Baskoutas, Chemical sensing applications of ZnO nanomaterials, Materials 11 (2018) 287, https://doi.org/10.3390/ma11020287 (Basel).
[37] S. Rackauskas, N. Barbero, C. Barolo, G. Viscardi, ZnO nanowire application in chemoresistive sensing: a review, Nanomaterials 7 (2017) 381, https://doi.org/10.3390/nano7110381.
[38] L. Zhu, W. Zeng, Room-temperature gas sensing of ZnO-based gas sensor: a review, Sens. Actuators A Phys. 267 (2017) 242–261, https://doi.org/10.1016/j.sna.2017.10.021.
[39] M. Yang, S. Zhang, F. Qu, S. Gong, C. Wang, L. Qiu, M. Yang, W. Cheng, High performance acetone sensor based on ZnO nanorods modified by Au nanoparticles, J. Alloys Compd. 797 (2019) 246–252, https://doi.org/10.1016/j.jallcom.2019.05.101.
[40] Y. Sun, H. Yang, Z. Zhao, K. Suematsu, P. Li, Z. Yu, W. Zhang, J. Hu, Fabrication of ZnO quantum dots@SnO_2 hollow nanospheres hybrid hierarchical structures for effectively detecting formaldehyde, Sens. Actuators B Chem. 318 (2020), 128222, https://doi.org/10.1016/j.snb.2020.128222.

[41] Z. Li, Z.J. Yao, A.A. Haidry, T. Plecenik, L.J. Xie, L.C. Sun, Q. Fatima, Resistive-type hydrogen gas sensor based on TiO_2: a review, Int. J. Hydrog. Energy (2018), https://doi.org/10.1016/j.ijhydene.2018.09.051.

[42] G. Velmathi, S. Mohan, R. Henry, Analysis and review of tin oxide-based chemoresistive gas sensor, IETE Tech. Rev. 33 (2016) 323–331, https://doi.org/10.1080/02564602.2015.1080603 (Institution Electron. Telecommun. Eng. India).

[43] L. Zhu, W. Zeng, Room-temperature gas sensing of ZnO-based gas sensor: a review, Sens. Actuators A Phys. 267 (2017) 242–261, https://doi.org/10.1016/j.sna.2017.10.021.

[44] R. Tang, Y. Shi, Z. Hou, L. Wei, Carbon nanotube-based chemiresistive sensors, Sensors 17 (2017) 882, https://doi.org/10.3390/s17040882.

[45] S. Ratan, C. Kumar, A. Kumar, D.K. Jarwal, A.K. Mishra, R.K. Upadhyay, S. Jit, Fabrication and characterization of a ZnO quantum dots-based metal–semiconductor–metal sensor for hydrogen gas, Nanotechnology 30 (2019), 395501, https://doi.org/10.1088/1361-6528/ab2c41.

[46] S. Samadi, M. Nouroozshad, S.A. Zakaria, ZnO@SiO2/rGO core/shell nanocomposite: a superior sensitive, selective and reproducible performance for 1-propanol gas sensor at room temperature, Mater. Chem. Phys. 271 (2021), 124884, https://doi.org/10.1016/j.matchemphys.2021.124884.

[47] J.H. Kim, A. Mirzaei, H.W. Kim, S.S. Kim, Low-Voltage-driven sensors based on ZnO nanowires for room-temperature detection of NO_2 and CO gases, ACS Appl. Mater. Interfaces 11 (2019) 24172–24183, https://doi.org/10.1021/acsami.9b07208.

[48] D.R. Miller, S.A. Akbar, P.A. Morris, Nanoscale metal oxide-based heterojunctions for gas sensing: a review, Sens. Actuators B Chem. 204 (2014) 250–272, https://doi.org/10.1016/j.snb.2014.07.074.

[49] Y. Kang, F. Yu, L. Zhang, W. Wang, L. Chen, Y. Li, Review of ZnO-based nanomaterials in gas sensors, Solid State Ionics 360 (2021), 115544, https://doi.org/10.1016/J.SSI.2020.115544.

[50] A. Bag, N.E. Lee, Gas sensing with heterostructures based on two-dimensional nanostructured materials: a review, J. Mater. Chem. C 7 (2019) 13367–13383, https://doi.org/10.1039/C9TC04132J.

[51] L.A. Mercante, R.S. Andre, L.H.C. Mattoso, D.S. Correa, Electrospun ceramic nanofibers and hybrid-nanofiber composites for gas sensing, ACS Appl. Nano Mater 2 (2019), https://doi.org/10.1021/acsanm.9b01176.

[52] T. Kerdcharoen, C. Wongchoosuk, Carbon nanotube and metal oxide hybrid materials for gas sensing, Semicond. Gas Sens. (2013) 386–407, https://doi.org/10.1533/9780857098665.3.386.

[53] Z.U. Abideen, J.H. Kim, J.H. Lee, J.Y. Kim, A. Mirzaei, H.W. Kim, S.S. Kim, Electrospun metal oxide composite nanofibers gas sensors: a review, J. Korean Ceram. Soc. 54 (2017) 366–379, https://doi.org/10.4191/kcers.2017.54.5.12.

[54] P.T. Moseley, Progress in the development of semiconducting metal oxide gas sensors: a review, Meas. Sci. Technol. 28 (2017), 082001, https://doi.org/10.1088/1361-6501/aa7443.

[55] A. Kusior, M. Radecka, M. Rekas, M. Lubecka, K. Zakrzewska, A. Reszka, B. J. Kowalski, Sensitization of gas sensing properties in TiO_2/SnO_2 nanocomposites, Procedia Eng. 47 (2012) 1073–1076, https://doi.org/10.1016/J.PROENG.2012.09.336.

[56] A. Chen, S. Bai, B. Shi, Z. Liu, D. Li, C.C. Liu, Methane gas-sensing and catalytic oxidation activity of SnO_2–In_2O_3 nanocomposites incorporating TiO_2, Sens. Actuators B Chem. 135 (2008) 7–12, https://doi.org/10.1016/J.SNB.2008.06.050.

[57] X. Yu, G. Zhang, H. Cao, X. An, Y. Wang, Z. Shu, X. An, F. Hua, ZnO@ZnS hollow dumbbells–graphene composites as high-performance photocatalysts and alcohol sensors, New J. Chem. 36 (2012) 2593–2598, https://doi.org/10.1039/C2NJ40770A.

[58] S.W. Choi, J.Y. Park, S.S. Kim, Synthesis of SnO2–ZnO core–shell nanofibers via a novel two-step process and their gas sensingproperties, Nanotechnology 20 (2009), 465603, https://doi.org/10.1088/0957-4484/20/46/465603.

[59] L. Wang, Y. Kang, Y. Wang, B. Zhu, S. Zhang, W. Huang, S. Wang, CuO nanoparticle decorated ZnO nanorod sensor for low-temperature H2S detection, Mater. Sci. Eng. C 32 (2012) 2079–2085, https://doi.org/10.1016/J.MSEC.2012.05.042.

[60] Y. Liu, G. Zhu, J. Chen, H. Xu, X. Shen, A. Yuan, Co_3O_4/ZnO nanocomposites for gas-sensing applications, Appl. Surf. Sci. 265 (2013) 379–384, https://doi.org/10.1016/j.apsusc.2012.11.016.

[61] W. Wang, Z. Li, W. Zheng, H. Huang, C. Wang, J. Sun, Cr_2O3-sensitized ZnO electrospun nanofibers based ethanol detectors, Sens. Actuators B Chem. 143 (2010) 754–758, https://doi.org/10.1016/J.SNB.2009.10.016.

[62] H. Gu, Z. Wang, Y. Hu, Hydrogen gas sensors based on semiconductor oxide nanostructures, Sensors 12 (12) (2012) 5517–5550, https://doi.org/10.3390/S120505517, 20125517–5550.

[63] M. Rumyantseva, V. Kovalenko, A. Gaskov, E. Makshina, V. Yuschenko, I. Ivanova, A. Ponzoni, G. Faglia, E. Comini, Nanocomposites SnO_2/Fe_2O_3: sensor and catalytic properties, Sens. Actuators B Chem. 118 (2006) 208–214, https://doi.org/10.1016/J.SNB.2006.04.024.

[64] B.P.J. De Lacy Costello, R.J. Ewen, N.M. Ratcliffe, P.S. Sivanand, Thick film organic vapour sensors based on binary mixtures of metal oxides, Sens. Actuators B Chem. 92 (2003) 159–166, https://doi.org/10.1016/S0925-4005(03)00258-2.

[65] A. Chen, X. Huang, Z. Tong, S. Bai, R. Luo, C.C. Liu, Preparation, characterization and gas-sensing properties of SnO_2–In_2O_3 nanocomposite oxides, Sens. Actuators B Chem. 115 (2006) 316–321, https://doi.org/10.1016/J.SNB.2005.09.015.

[66] C. Liangyuan, B. Shouli, Z. Guojun, L. Dianqing, C. Aifan, C.C. Liu, Synthesis of ZnO–SnO_2 nanocomposites by microemulsion and sensing properties for NO_2, Sens. Actuators B Chem. 134 (2008) 360–366, https://doi.org/10.1016/J.SNB.2008.04.040.

[67] Y. Zeng, Y.F. Bing, C. Liu, W.T. Zheng, G.T. Zou, Self-assembly of hierarchical $ZnSnO_3$-SnO_2 nanoflakes and their gas sensing properties, Trans. Nonferrous Met. Soc. China. 22 (2012) 2451–2458, https://doi.org/10.1016/S1003-6326(11)61484-2.

[68] A. Wei, L. Pan, W. Huang, Recent progress in the ZnO nanostructure-based sensors, Mater. Sci. Eng. B 176 (2011) 1409–1421, https://doi.org/10.1016/j.mseb.2011.09.005.

[69] P. Pascariu, M. Homocianu, ZnO-based ceramic nanofibers: Preparation, properties and applications, Ceram. Int. 45 (2019) 11158–11173, https://doi.org/10.1016/j.ceramint.2019.03.113.

[70] X. Xiao, L. Liu, J. Ma, Y. Ren, X. Cheng, Y. Zhu, D. Zhao, A.A. Elzatahry, A. Alghamdi, Y. Deng, Ordered mesoporous tin oxide semiconductors with large pores and crystallized walls for high-performance gas sensing, ACS Appl. Mater. Interfaces 10 (2018) 1871–1880, https://doi.org/10.1021/acsami.7b18830.

[71] A. Dey, Semiconductor metal oxide gas sensors: a review, Mater. Sci. Eng. B Solid State Mater. Adv. Technol. 229 (2018) 206–217, https://doi.org/10.1016/j.mseb.2017.12.036.

[72] P. Shankar, J. Rayappan, Gas sensing mechanism of metal oxides: the role of ambient atmosphere, type of semiconductor and gases-a review, ScienceJet 4 (2015) 1–18.

[73] H. Ji, W. Zeng, Y. Li, Gas sensing mechanisms of metal oxide semiconductors: a focus review, Nanoscale 11 (2019) 22664–22684, https://doi.org/10.1039/C9NR07699A.

[74] Z.S. Hosseini, A.I. Zad, A. Mortezaali, Room temperature H2S gas sensor based on rather aligned ZnO nanorods with flower-like structures, Sens. Actuators B Chem. 207 (2015) 865–871, https://doi.org/10.1016/j.snb.2014.10.085.

[75] A. Katoch, G.J. Sun, S.W. Choi, J.H. Byun, S.S. Kim, Competitive influence of grain size and crystallinity on gas sensing performances of ZnO nanofibers, Sens. Actuators B Chem. 185 (2013) 411–416, https://doi.org/10.1016/j.snb.2013.05.030.

[76] J.G. Lu, P. Chang, Z. Fan, Quasi-one-dimensional metal oxide materials—synthesis, properties and applications, Mater. Sci. Eng. R Rep. 52 (2006) 49–91, https://doi.org/10.1016/J.MSER.2006.04.002.

[77] Y.W. Heo, D.P. Norton, L.C. Tien, Y. Kwon, B.S. Kang, F. Ren, S.J. Pearton, J. R. Laroche, ZnO nanowire growth and devices, Mater. Sci. Eng. R Rep. 47 (2004) 1–47, https://doi.org/10.1016/J.MSER.2004.09.001.

[78] Z. Fan, J.G. Lu, Zinc oxide nanostructures: synthesis and properties, J. Nanosci. Nanotechnol. 5 (2005) 1561–1573, https://doi.org/10.1166/JNN.2005.182.

[79] N.A. Abdullah, Z. Khusaimi, M. Rusop, A review on zinc oxide nanostructures: doping and gas sensing, Adv. Mater. Res. 667 (2013) 329–332, https://doi.org/10.4028/WWW.SCIENTIFIC.NET/AMR.667.329.

[80] D. Nunes, A. Pimentel, A. Goncalves, S. Pereira, R. Branquinho, P. Barquinha, E. Fortunato, R. Martins, Metal oxide nanostructures for sensor applications, Semicond. Sci. Technol. 34 (2019), 043001, https://doi.org/10.1088/1361-6641/AB011E.

[81] Z.L. Wang, Zinc oxide nanostructures: growth, properties and applications, J. Phys. Condens. Matter. 16 (2004) R829, https://doi.org/10.1088/0953-8984/16/25/R01.

[82] L. Schmidt-Mende, J.L. MacManus-Driscoll, ZnO – nanostructures, defects, and devices, Mater. Today 10 (2007) 40–48, https://doi.org/10.1016/S1369-7021(07)70078-0.

[83] A. Kolodziejczak-Radzimska, T. Jesionowski, Zinc oxide—from synthesis to application: a review, Materials 7 (2014) 2833–2881, https://doi.org/10.3390/MA7042833, 201472833–2881.

[84] K. Lim, M.A.A. Hamid, R. Shamsudin, N.H. Al-Hardan, I. Mansor, W. Chiu, Temperature-driven structural and morphological evolution of zinc oxide nano-coalesced microstructures and its defect-related photoluminescence properties, Materials 9 (2016) 300, https://doi.org/10.3390/MA9040300, 2016Page9300.

[85] Ü. Özgür, Y.I. Alivov, C. Liu, A. Teke, M.A. Reshchikov, S. Doğan, V. Avrutin, S. J. Cho, H. Morkç, A comprehensive review of ZnO materials and devices, J. Appl. Phys. 98 (2005), 041301, https://doi.org/10.1063/1.1992666.

[86] Y. Jia, K. Jiang, H. Wang, X. Yao, The Role of Defect Sites in Nanomaterials for Electrocatalytic Energy Conversion, Chem 5 (2019) 1371–1397, https://doi.org/10.1016/J.CHEMPR.2019.02.008.

[87] W.J. Lee, J. Lim, S.O. Kim, Nitrogen dopants in carbon nanomaterials: defects or a new opportunity? Small Methods 1 (2017), 1600014 https://doi.org/10.1002/SMTD.201600014.

[88] Zinc oxide: perfect pair of defects, NPG Asia Mater. 2009 (2009) 1, https://doi.org/10.1038/asiamat.2009.216. –1.

[89] H. Zeng, G. Duan, Y. Li, S. Yang, X. Xu, W. Cai, Blue luminescence of ZnO nanoparticles based on non-equilibrium processes: defect origins and emission controls, Adv. Funct. Mater. 20 (2010) 561–572, https://doi.org/10.1002/ADFM.200901884.

[90] Zinc oxide: Perfect pair of defects, NPG Asia Mater. 2009. (2009) 11. doi:10.1038/asiamat.2009.216.

[91] H. Zeng, G. Duan, Y. Li, S. Yang, X. Xu, W. Cai, Blue Luminescence of ZnO Nanoparticles Based on Non-Equilibrium Processes: Defect Origins and Emission Controls, Adv. Funct. Mater. 20 (2010) 561–572, https://doi.org/10.1002/ADFM.200901884.

[92] D.H. Kim, G.W. Lee, Y.C. Kim, Interaction of zinc interstitial with oxygen vacancy in zinc oxide: an origin of n-type doping, Solid State Commun. 152 (2012) 1711–1714, https://doi.org/10.1016/J.SSC.2012.06.016.

[93] F. Oba, M. Choi, A. Togo, I. Tanaka, Point defects in ZnO: an approach from first principles, Sci. Technol. Adv. Mater. 12 (2011), 034302, https://doi.org/10.1088/1468-6996/12/3/034302.

[94] V. Ischenko, S. Polarz, D. Grote, V. Stavarache, K. Fink, M. Driess, Zinc oxide nanoparticles with defects, Adv. Funct. Mater. 15 (2005) 1945–1954, https://doi.org/10.1002/ADFM.200500087.

[95] J. Zhang, X. Liu, G. Neri, N. Pinna, Nanostructured materials for room-temperature gas sensors, Adv. Mater. 28 (2016) 795–831, https://doi.org/10.1002/adma.201503825.

[96] D. Brunelli, M. Rossi, Enhancing lifetime of WSN for natural gas leakages detection, Microelectron. J. 45 (2014) 1665–1670, https://doi.org/10.1016/j.mejo.2014.08.006.

[97] J.S. Caygill, F. Davis, S.P.J. Higson, Current trends in explosive detection techniques, Talanta 88 (2012) 14–29, https://doi.org/10.1016/j.talanta.2011.11.043.

[98] H. Farahani, R. Wagiran, M.N. Hamidon, Humidity sensors principle, mechanism, and fabrication technologies: a comprehensive review, Sensors 14 (2014) 7881–7939, https://doi.org/10.3390/S140507881, 2014147881–7939.

[99] A. Alkahlout, N. Al Dahoudi, I. Grobelsek, M. Jilavi, P.W. de Oliveira, Synthesis and characterization of aluminum doped zinc oxide nanostructures via hydrothermal route, J. Mater. 2014 (2014) 1–8, https://doi.org/10.1155/2014/235638.

[100] P.K. Shihabudeen, M.Y. Notash, J.J. Sardroodi, A.R Chaudhuri, Nitrogen incorporated zinc oxide thin film for efficient ethanol detection, Sens. Actuators B Chem. 358 (2022), 131544, https://doi.org/10.1016/j.snb.2022.131544.

[101] B.J. Skromme, G.K. Sujan, Semiconductor heterojunctions, Ref. Modul. Mater. Sci. Mater. Eng. (2018), https://doi.org/10.1016/B978-0-12-803581-8.11219-6.

[102] G. Shao, G. Shao, Work function and electron affinity of semiconductors: doping effect and complication due to fermi level pinning, Energy Environ. Mater. 4 (2021) 273–276, https://doi.org/10.1002/EEM2.12218.

[103] R.T. Bueno, O.F. Lopes, K.T.G. Carvalho, C. Ribeiro, H.A.J.L. Mouraõ, Semicondutores heteroestruturados: Uma abordagem sobre os principais desafios para a obtenção e aplicação em processos fotoquímicos ambientais e energéticos, Quim. Nova 42 (2019) 661–675, https://doi.org/10.21577/0100-4042.20170372.

[104] K.C. Hsu, T.H. Fang, Y.J. Hsiao, Z.J. Li, Rapid detection of low concentrations of H2S using CuO-doped ZnO nanofibers, J. Alloys Compd. 852 (2021), 157014, https://doi.org/10.1016/j.jallcom.2020.157014.

[105] Z. Qu, Y. Fu, B. Yu, P. Deng, L. Xing, X. Xue, High and fast H2S response of NiO/ZnO nanowire nanogenerator as a self-powered gas sensor, Sens. Actuators B Chem. 222 (2016) 78–86, https://doi.org/10.1016/J.SNB.2015.08.058.

[106] N. Jayababu, M. Poloju, J. Shruthi, M.V.R. Reddy, Synthesis of ZnO/NiO nanocomposites for the rapid detection of ammonia at room temperature, Mater. Sci. Semicond. Process. 102 (2019), 104591, https://doi.org/10.1016/J.MSSP.2019.104591.

[107] R.S. Andre, J.C. Pereira, L.A. Mercante, D. Locilento, L.H.C. Mattoso, D.S. Correa, ZnO-Co_3O_4 heterostructure electrospun nanofibers modified with poly(sodium 4-styrenesulfonate): evaluation of humidity sensing properties, J. Alloys Compd. 767 (2018) 1022–1029, https://doi.org/10.1016/j.jallcom.2018.07.132.

[108] S. Park, Enhancement of hydrogen sensing response of ZnO nanowires for the decoration of WO_3 nanoparticles, Mater. Lett. 234 (2019) 315–318, https://doi.org/10.1016/j.matlet.2018.09.129.

[109] B. Mondal, B. Basumatari, J. Das, C. Roychaudhury, H. Saha, N. Mukherjee, ZnO–SnO_2 based composite type gas sensor for selective hydrogen sensing, Sens. Actuators B Chem. 194 (2014) 389–396, https://doi.org/10.1016/j.snb.2013.12.093.

[110] X. Song, L. Li, X. Chen, Q. Xu, B. Song, Z. Pan, Y. Liu, F. Juan, F. Xu, B. Cao, Enhanced triethylamine sensing performance of α-Fe2O3 nanoparticle/ZnO nanorod heterostructures, Sens. Actuators B Chem. 298 (2019), 126917, https://doi.org/10.1016/j.snb.2019.126917.

[111] S.I. Boyadjiev, O. Kéri, P. Bárdos, T. Firkala, F. Gáber, Z.K. Nagy, Z. Baji, M. Takács, I.M. Szilágyi, TiO_2/ZnO and ZnO/TiO_2 core/shell nanofibers prepared by electrospinning and atomic layer deposition for photocatalysis and gas sensing, Appl. Surf. Sci. 424 (2017) 190–197, https://doi.org/10.1016/j.apsusc.2017.03.030.

[112] R.S. Andre, Q.P. Ngo, L. Fugikawa-Santos, D.S. Correa, T.M. Swager, Wireless tags with hybrid nanomaterials for volatile amine detection, ACS Sens. 6 (2021) 2457–2464, https://doi.org/10.1021/acssensors.1c00812.

[113] R.S. Andre, K. Campaner, M.H.M. Facure, L.A. Mercante, S. Bogusz, D.S. Correa, Nanocomposite-based chemiresistive electronic nose and application in coffee analysis, ACS Food Sci. Technol. 1 (2021) 1464–1471, https://doi.org/10.1021/acsfoodscitech.1c00173.

[114] R.S. Andre, F.M. Shimizu, C.M. Miyazaki, A. Riul, D. Manzani, S.J.L. Ribeiro, O. N. Oliveira, L.H.C. Mattoso, D.S. Correa, Hybrid layer-by-layer (LbL) films of polyaniline, graphene oxide and zinc oxide to detect ammonia, Sens. Actuators B Chem. 238 (2017) 795–801, https://doi.org/10.1016/j.snb.2016.07.099.

[115] R. Yatskiv, J. Grym, S. Tiagulskyi, N. Bašinová, Influence of surface polarity on optoelectronic properties of PEDOT:PSS/ZnO hybrid heterojunctions, Phys. Status Solidi. 218 (2021), 2000612, https://doi.org/10.1002/pssa.202000612.

[116] H. Du, W. Yang, W. Yi, Y. Sun, N. Yu, J. Wang, Oxygen-plasma-assisted enhanced acetone-sensing properties of ZnO nanofibers by electrospinning, ACS Appl. Mater. Interfaces 12 (2020) 23084–23093, https://doi.org/10.1021/acsami.0c03498.

[117] J.C. Fan, K.M. Sreekanth, Z. Xie, S.L. Chang, K.V. Rao, p-Type ZnO materials: theory, growth, properties and devices, Prog. Mater. Sci. 58 (2013) 874–985, https://doi.org/10.1016/J.PMATSCI.2013.03.002.

[118] Y. Chen, Z. Shen, Q. Jia, J. Zhao, Z. Zhao, H. Ji, A CuO–ZnO nanostructured p–n junction sensor for enhanced N-butanol detection, RSC Adv. 6 (2015) 2504–2511, https://doi.org/10.1039/C5RA20031H.

[119] G. Dai, S. Liu, Y. Liang, T. Luo, Synthesis and enhanced photoelectrocatalytic activity of p–n junction Co_3O_4/TiO_2 nanotube arrays, Appl. Surf. Sci. 264 (2013) 157–161, https://doi.org/10.1016/J.APSUSC.2012.09.160.

[120] B. Roul, M. Kumar, M.K. Rajpalke, T.N. Bhat, S.B. Krupanidhi, Binary group III-nitride based heterostructures: band offsets and transport properties, J. Phys. D. Appl. Phys. 48 (2015), 423001, https://doi.org/10.1088/0022-3727/48/42/423001.

[121] J. Ge, Y. Zhang, Y.J. Heo, S.J. Park, Advanced design and synthesis of composite photocatalysts for the remediation of wastewater: a review, Catalysts 9 (2019) 122, https://doi.org/10.3390/CATAL9020122, 2019Page9122.

[122] Z. Wang, L. Zhu, S. Sun, J. Wang, W. Yan, One-dimensional nanomaterials in resistive gas sensor: from material design to application, Chemosensors 9 (2021) 198, https://doi.org/10.3390/CHEMOSENSORS9080198. Page9 (2021) 198.

[123] M.S. Whittingham, Hydrothermal synthesis of transition metal oxides under mild conditions, Curr. Opin. Solid State Mater. Sci. 1 (1996) 227–232, https://doi.org/10.1016/S1359-0286(96)80089-1.

[124] H.C. Hailes, Reaction solvent selection: the potential of water as a solvent for organic transformations, Org. Process Res. Dev. 11 (2006) 114–120, https://doi.org/10.1021/OP060157X.

[125] T.H. Chang, Y.C. Lu, M.J. Yang, J.W. Huang, P.F. Linda Chang, H.Y. Hsueh, Multibranched flower-like ZnO particles from eco-friendly hydrothermal synthesis as green antimicrobials in agriculture, J. Clean. Prod. 262 (2020), 121342, https://doi.org/10.1016/J.JCLEPRO.2020.121342.

[126] Q. Zhang, K. Zhang, D. Xu, G. Yang, H. Huang, F. Nie, C. Liu, S. Yang, CuO nanostructures: synthesis, characterization, growth mechanisms, fundamental properties, and applications, Prog. Mater. Sci. 60 (2014) 208–337, https://doi.org/10.1016/J.PMATSCI.2013.09.003.

[127] A. Rydosz, The use of copper oxide thin films in gas-sensing applications, Coatings 8 (2018) 425, https://doi.org/10.3390/COATINGS8120425, 2018Page8425.

[128] T. Okamoto, S. Kumagai, E. Fukuzaki, H. Ishii, G. Watanabe, N. Niitsu, T. Annaka, M. Yamagishi, Y. Tani, H. Sugiura, T. Watanabe, S. Watanabe, J. Takeya, Robust, high-performance n-type organic semiconductors, Sci. Adv. 6 (2020), https://doi.org/10.1126/SCIADV.AAZ0632/SUPPL_FILE/AAZ0632_SM.PDF.

[129] A. Goldoni, V. Alijani, L. Sangaletti, L. D'Arsiè, Advanced promising routes of carbon/metal oxides hybrids in sensors: a review, Electrochim. Acta 266 (2018) 139–150, https://doi.org/10.1016/J.ELECTACTA.2018.01.170.

[130] A. Koo, R. Yoo, S.P. Woo, H.S. Lee, W. Lee, Enhanced acetone-sensing properties of Pt-decorated al-doped ZnO nanoparticles, Sens. Actuators B Chem. 280 (2019) 109–119, https://doi.org/10.1016/j.snb.2018.10.049.

[131] J. Guo, J. Zhang, M. Zhu, D. Ju, H. Xu, B. Cao, High-performance gas sensor based on ZnO nanowires functionalized by Au nanoparticles, Sens. Actuators B Chem. 199 (2014) 339–345, https://doi.org/10.1016/j.snb.2014.04.010.

[132] R. Yoo, S. Cho, M.J. Song, W. Lee, Highly sensitive gas sensor based on Al-doped ZnO nanoparticles for detection of dimethyl methylphosphonate as a chemical warfare agent simulant, Sens. Actuators B Chem. 221 (2015) 217–223, https://doi.org/10.1016/j.snb.2015.06.076.

[133] N. Dwivedi, S. Kumar, H.K. Malik, C.M.S.R Govind, O.S. Panwar, Correlation of sp3 and sp2 fraction of carbon with electrical, optical and nano-mechanical properties of argon-diluted diamond-like carbon films, Appl. Surf. Sci. 257 (2011) 6804–6810, https://doi.org/10.1016/J.APSUSC.2011.02.134.

[134] Q. Yuan, C. Te Lin, K.W.A. Chee, All-carbon devices based on sp2-on-sp3 configuration, APL Mater. 7 (2019), 030901, https://doi.org/10.1063/1.5082767.

[135] J. Watson, The tin oxide gas sensor and its applications, Sens. Actuators 5 (1984) 29–42, https://doi.org/10.1016/0250-6874(84)87004-3.

[136] Z. Jing, J. Zhan, Fabrication and gas-sensing properties of porous ZnO nanoplates, Adv. Mater. 20 (2008) 4547–4551, https://doi.org/10.1002/ADMA.200800243.

[137] C. Liu, L. Zhao, B. Wang, P. Sun, Q. Wang, Y. Gao, X. Liang, T. Zhang, G. Lu, Acetone gas sensor based on NiO/ZnO hollow spheres: fast response and recovery, and low (ppb) detection limit, J. Colloid Interface Sci. 495 (2017) 207–215, https://doi.org/10.1016/J.JCIS.2017.01.106.

[138] R.K. Sonker, S.R. Sabhajeet, S. Singh, B.C. Yadav, Synthesis of ZnO nanopetals and its application as NO_2 gas sensor, Mater. Lett. 152 (2015) 189–191, https://doi.org/10.1016/J.MATLET.2015.03.112.

[139] V. Najafi, S. Zolghadr, S. Kimiagar, Remarkable reproducibility and significant sensitivity of ZnO nanoparticles covered by Chromium (III) oxide as a hydrogen sulfide gas sensor, Optik 182 (2019) 249–256, https://doi.org/10.1016/j.ijleo.2019.01.015 (Stuttg).

[140] L. Zhu, Y. Li, W. Zeng, Hydrothermal synthesis of hierarchical flower-like ZnO nanostructure and its enhanced ethanol gas-sensing properties, Appl. Surf. Sci. 427 (2018) 281–287, https://doi.org/10.1016/j.apsusc.2017.08.229.

[141] X. Hu, M. Wang, J. Deng, S. ul H. Bakhtiar, Z. Zheng, W. Luo, W. Dong, Q. Fu, Sensing properties and mechanism of gas sensors based on zinc oxide quantum dots, IEEE Sens. J. 21 (2021) 19722–19730, https://doi.org/10.1109/JSEN.2021.3098002.

[142] B. Selvaraj, J.B. Balaguru Rayappan, K.J. Babu, Influence of calcination temperature on the growth of electrospun multi-junction ZnO nanowires: a room temperature ammonia sensor, Mater. Sci. Semicond. Process. 112 (2020), 105006, https://doi.org/10.1016/j.mssp.2020.105006.

[143] Y. Al-Hadeethi, A. Umar, A.A. Ibrahim, S.H. Al-Heniti, R. Kumar, S. Baskoutas, B. M. Raffah, Synthesis, characterization and acetone gas sensing applications of Ag-doped ZnO nanoneedles, Ceram. Int. 43 (2017) 6765–6770, https://doi.org/10.1016/j.ceramint.2017.02.088.

[144] J. Gonzalez-Chavarri, L. Parellada-Monreal, I. Castro-Hurtado, E. Castaño, G. G. Mandayo, ZnO nanoneedles grown on chip for selective NO_2 detection indoors, Sens. Actuators B Chem. 255 (2018) 1244–1253, https://doi.org/10.1016/j.snb.2017.08.094.
[145] Q. Li, D. Chen, J. Miao, S. Lin, Z. Yu, D. Cui, Z. Yang, X. Chen, Highly sensitive sensor based on ordered porous ZnO nanosheets for ethanol detecting application, Sens. Actuators B Chem. 326 (2021), 128952, https://doi.org/10.1016/j.snb.2020.128952.
[146] Y. Nagarjuna, Y.J. Hsiao, Au doping ZnO nanosheets sensing properties of ethanol gas prepared on MEMS device, Coatings 10 (2020) 945, https://doi.org/10.3390/coatings10100945.
[147] M. Kumar, V. Bhatt, J. Kim, A.C. Abhyankar, H.J. Chung, K. Singh, Y. Bin Cho, Y. J. Yun, K.S. Lim, J.H. Yun, Holey engineered 2D ZnO-nanosheets architecture for supersensitive ppm level H2 gas detection at room temperature, Sens. Actuators B Chem. 326 (2021), 128839, https://doi.org/10.1016/j.snb.2020.128839.
[148] S. Shao, X. Chen, Y. Chen, L. Zhang, H.W. Kim, S.S. Kim, ZnO nanosheets modified with graphene quantum dots and SnO_2 quantum nanoparticles for room-temperature H_2S sensing, ACS Appl. Nano Mater. 3 (2020) 5220–5230, https://doi.org/10.1021/acsanm.0c00642.
[149] J.H. Kim, A. Mirzaei, M. Osada, H.W. Kim, S.S. Kim, Hydrogen sensing characteristics of Pd-decorated ultrathin ZnO nanosheets, Sens. Actuators B Chem. 329 (2021), 129222, https://doi.org/10.1016/j.snb.2020.129222.
[150] H. Chen, C. Li, X. Zhang, W. Yang, ZnO nanoplates with abundant porosity for significant formaldehyde-sensing, Mater. Lett. 260 (2020), 126982, https://doi.org/10.1016/j.matlet.2019.126982.
[151] L. Van Duy, T.T. Nguyet, C.M. Hung, D.T. Thanh Le, N. Van Duy, N.D. Hoa, F. Biasioli, M. Tonezzer, C. Di Natale, Ultrasensitive NO_2 gas sensing performance of two dimensional ZnO nanomaterials: nanosheets and nanoplates, Ceram. Int. 47 (2021) 28811–28820, https://doi.org/10.1016/j.ceramint.2021.07.042.
[152] Y. Song, F. Chen, Y. Zhang, S. Zhang, F. Liu, P. Sun, X. Yan, G. Lu, Fabrication of highly sensitive and selective room-temperature nitrogen dioxide sensors based on the ZnO nanoflowers, Sens. Actuators B Chem. 287 (2019) 191–198, https://doi.org/10.1016/j.snb.2019.01.146.
[153] S. Agarwal, P. Rai, E.N. Gatell, E. Llobet, F. Güell, M. Kumar, K. Awasthi, Gas sensing properties of ZnO nanostructures (flowers/rods) synthesized by hydrothermal method, Sens. Actuators B Chem. 292 (2019) 24–31, https://doi.org/10.1016/j.snb.2019.04.083.
[154] V. Galstyan, Quantum dots: perspectives in next-generation chemical gas sensors" – a review, Anal. Chim. Acta 1152 (2021), 238192, https://doi.org/10.1016/j.aca.2020.12.067.
[155] B. Baruwati, D.K. Kumar, S.V. Manorama, Hydrothermal synthesis of highly crystalline ZnO nanoparticles: a competitive sensor for LPG and EtOH, Sens. Actuators B Chem. 119 (2006) 676–682, https://doi.org/10.1016/j.snb.2006.01.028.
[156] P. Rai, Y.T. Yu, Citrate-assisted hydrothermal synthesis of single crystalline ZnO nanoparticles for gas sensor application, Sens. Actuators B Chem. 173 (2012) 58–65, https://doi.org/10.1016/j.snb.2012.05.068.
[157] S. Jaballah, M. Benamara, H. Dahman, A. Ly, D. Lahem, M. Debliquy, L. El Mir, Effect of Mg-doping ZnO nanoparticles on detection of low ethanol concentrations, Mater. Chem. Phys. 255 (2020), 123643, https://doi.org/10.1016/j.matchemphys.2020.123643.
[158] G. Niarchos, G. Dubourg, G. Afroudakis, M. Georgopoulos, V. Tsouti, E. Makarona, V. Crnojevic-Bengin, C. Tsamis, Humidity sensing properties of paper substrates and their passivation with ZnO nanoparticles for sensor applications, Sensors 17 (2017) 516, https://doi.org/10.3390/s17030516.
[159] H.R. Yousefi, B. Hashemi, A. Mirzaei, H. Roshan, M.H. Sheikhi, Effect of Ag on the ZnO nanoparticles properties as an ethanol vapor sensor, Mater. Sci. Semicond. Process. 117 (2020), 105172, https://doi.org/10.1016/j.mssp.2020.105172.
[160] Y. Li, M. Jiao, H. Zhao, M. Yang, High performance gas sensors based on in-situ fabricated ZnO/polyaniline nanocomposite: the effect of morphology on the sensing properties, Sens. Actuators B Chem. 264 (2018) 285–295, https://doi.org/10.1016/j.snb.2018.02.157.
[161] A. Ryzhikov, J. Jońca, M. Kahn, K. Fajerwerg, B. Chaudret, A. Chapelle, P. Ménini, C.H. Shim, A. Gaudon, P. Fau, Organometallic synthesis of ZnO nanoparticles for gas sensing: towards selectivity through nanoparticles morphology, J. Nanoparticle Res. 17 (2015) 280, https://doi.org/10.1007/s11051-015-3086-2.
[162] B. Gidwani, V. Sahu, S.S. Shukla, R. Pandey, V. Joshi, V.K. Jain, A. Vyas, Quantum dots: prospectives, toxicity, advances and applications, J. Drug Deliv. Sci. Technol. 61 (2021), 102308, https://doi.org/10.1016/j.jddst.2020.102308.
[163] Y. Park, R. Yoo, S. ryull Park, J.H. Lee, H. Jung, H.S. Lee, W. Lee, Highly sensitive and selective isoprene sensing performance of ZnO quantum dots for a breath analyzer, Sens. Actuators B Chem. 290 (2019) 258–266, https://doi.org/10.1016/j.snb.2019.03.118.
[164] S. Zhai, H.E. Karahan, C. Wang, Z. Pei, L. Wei, Y. Chen, 1D supercapacitors for emerging electronics: current status and future directions, Adv. Mater. 32 (2020), 1902387, https://doi.org/10.1002/adma.201902387.
[165] M. Samadi, M. Zirak, A. Naseri, M. Kheirabadi, M. Ebrahimi, A.Z. Moshfegh, Design and tailoring of one-dimensional ZnO nanomaterials for photocatalytic degradation of organic dyes: a review, Res. Chem. Intermed. 45 (2019) 2197–2254, https://doi.org/10.1007/s11164-018-03729-5.
[166] Y. He, B. Matthews, J. Wang, L. Song, X. Wang, G. Wu, Innovation and challenges in materials design for flexible rechargeable batteries: from 1D to 3D, J. Mater. Chem. A 6 (2018) 735–753, https://doi.org/10.1039/C7TA09301B.
[167] B. Yang, N.V. Myung, T. Tran, 1D metal oxide semiconductor materials for chemiresistive gas sensors: a review, Adv. Electron. Mater. 7 (2021), 2100271, https://doi.org/10.1002/aelm.202100271.
[168] B.W.S. Vijayakumar, C. Manjunatha, B. Abhishek, G. Nagaraju, P.K. Panda, Hydrothermal synthesis of ZnO nanotubes for CO gas sensing, Sens. Int. 1 (2020), 100018, https://doi.org/10.1016/j.sintl.2020.100018.
[169] J.X. Wang, X.W. Sun, Y. Yang, C.M.L. Wu, N–P transition sensing behaviors of ZnO nanotubes exposed to NO_2 gas, Nanotechnology 20 (2009), 465501, https://doi.org/10.1088/0957-4484/20/46/465501.
[170] O.S. Kwon, H.S. Song, T.H. Park, J. Jang, Conducting nanomaterial sensor using natural receptors, Chem. Rev. 119 (2019) 36–93, https://doi.org/10.1021/acs.chemrev.8b00159.
[171] S. Zhao, Y. Shen, P. Zhou, F. Hao, X. Xu, S. Gao, D. Wei, Y. Ao, Y. Shen, Enhanced NO_2 sensing performance of ZnO nanowires functionalized with ultra-fine In_2O_3 nanoparticles, Sens. Actuators B Chem. 308 (2020), 127729, https://doi.org/10.1016/j.snb.2020.127729.
[172] P. Srinivasan, J.B.B. Rayappan, Growth of Eshelby twisted ZnO nanowires through nanoflakes & nanoflowers: a room temperature ammonia sensor, Sens. Actuators B Chem. 277 (2018) 129–143, https://doi.org/10.1016/j.snb.2018.09.003.
[173] Y. Luo, A. Ly, D. Lahem, C. Zhang, M. Debliquy, A novel low-concentration isopropanol gas sensor based on Fe-doped ZnO nanoneedles and its gas sensing mechanism, J. Mater. Sci. 56 (2021) 3230–3245, https://doi.org/10.1007/s10853-020-05453-1.
[174] A.J. Bandari, S. Nasirian, Carbon monoxide gas sensing features of zinc oxide nanoneedles: practical selectivity and long-term stability, J. Mater. Sci. Mater. Electron. 30 (2019) 10073–10081, https://doi.org/10.1007/s10854-019-01111-8.
[175] C. Li, Z. Du, H. Yu, T. Wang, Low-temperature sensing and high sensitivity of ZnO nanoneedles due to small size effect, Thin. Solid Films 517 (2009) 5931–5934, https://doi.org/10.1016/j.tsf.2009.04.025.
[176] A. Aziz, N. Tiwale, S.A. Hodge, S.J. Attwood, G. Divitini, M.E. Welland, Core–shell electrospun polycrystalline ZnO nanofibers for ultra-sensitive NO_2 gas sensing, ACS Appl. Mater. Interfaces 10 (2018) 43817–43823, https://doi.org/10.1021/acsami.8b17149.
[177] J.H. Lee, J.Y. Kim, A. Mirzaei, H. Kim, S. Kim, Significant enhancement of hydrogen-sensing properties of ZnO nanofibers through NiO loading, Nanomaterials 8 (2018) 902, https://doi.org/10.3390/nano8110902.
[178] J.H. Lee, J.Y. Kim, J.H. Kim, S. Kim, Enhanced Hydrogen Detection in ppb-Level by Electrospun SnO2-Loaded ZnO Nanofibers, Sensors 19 (2019) 726, https://doi.org/10.3390/s19030726.
[179] J.H. Kim, A. Mirzaei, H.W Kim, P. Wu, S.S. Kim, Design of supersensitive and selective ZnO-nanofiber-based sensors for H2 gas sensing by electron-beam irradiation, Sens. Actuators B Chem. 293 (2019) 210–223, https://doi.org/10.1016/j.snb.2019.04.113.
[180] A.P. Dral, J.E. ten Elshof, 2D metal oxide nanoflakes for sensing applications: Review and perspective, Sens. Actuators B Chem. 272 (2018) 369–392, https://doi.org/10.1016/j.snb.2018.05.157.
[181] Y. Wang, X. Meng, J. Cao, Rapid detection of low concentration CO using Pt-loaded ZnO nanosheets, J. Hazard. Mater. 381 (2020), 120944, https://doi.org/10.1016/j.jhazmat.2019.120944.
[182] C.M. Hung, L. Van Duy, D.T. Thanh Le, H. Nguyen, N. Van Duy, N.D. Hoa, ZnO coral-like nanoplates decorated with Pd nanoparticles for enhanced VOC gas sensing, J. Sci. Adv. Mater. Devices 6 (2021) 453–461, https://doi.org/10.1016/j.jsamd.2021.05.005.
[183] Z. Yuan, Z. Feng, L. Kong, J. Zhan, X. Ma, Simple synthesis of porous ZnO nanoplates hyper-doped with low concentration of Pt for efficient acetone sensing, J. Alloys Compd. 865 (2021), 158890, https://doi.org/10.1016/j.jallcom.2021.158890.
[184] B. Jiang, J. Lu, W. Han, Y. Sun, Y. Wang, P. Cheng, H. Zhang, C. Wang, G. Lu, Hierarchical mesoporous zinc oxide microspheres for ethanol gas sensor, Sens. Actuators B Chem. 357 (2022), 131333, https://doi.org/10.1016/j.snb.2021.131333.
[185] G. Lo Sciuto, P. Kałużyński, S. Coco, 3D finite element simulation model of a chemiresistor gas sensor based on ZnO and graft comb copolymer integrated in a gas chamber, J. Mater. Sci. Mater. Electron. 33 (2022) 5037–5048, https://doi.org/10.1007/s10854-022-07692-1.
[186] J. Bruce, K. Bosnick, E.K Heidari, Pd-decorated ZnO nanoflowers as a promising gas sensor for the detection of meat spoilage, Sens. Actuators B Chem. 355 (2022), 131316, https://doi.org/10.1016/j.snb.2021.131316.
[187] X. Wang, M. Ahmad, H. Sun, Three-dimensional ZnO hierarchical nanostructures: solution phase synthesis and applications, Materials 10 (2017) 1304, https://doi.org/10.3390/ma10111304 (Basel).
[188] S. Zhang, C. Wang, F. Qu, S. Liu, C.T. Lin, S. Du, Y. Chen, F. Meng, M. Yang, ZnO nanoflowers modified with RuO_2 for enhancing acetone sensing performance, Nanotechnology 31 (2020), 115502, https://doi.org/10.1088/1361-6528/ab5cd9.
[189] H. Zhang, J. Yi, Enhanced ethanol gas sensing performance of ZnO nanoflowers decorated with $LaMnO_3$ perovskite nanoparticles, Mater. Lett. 216 (2018) 196–198, https://doi.org/10.1016/j.matlet.2018.01.018.
[190] R. Jaisutti, M. Lee, J. Kim, S. Choi, T.J. Ha, J. Kim, H. Kim, S.K. Park, Y.H. Kim, Ultrasensitive room-temperature operable gas sensors using p-type Na:ZnO nanoflowers for diabetes detection, ACS Appl. Mater. Interfaces 9 (2017) 8796–8804, https://doi.org/10.1021/acsami.7b00673.
[191] J.Y. Jeon, S.J. Park, T.J. Ha, Functionalization of zinc oxide nanoflowers with palladium nanoparticles via microwave absorption for room temperature-

operating hydrogen gas sensors in the ppb level, ACS Appl. Mater. Interfaces 13 (2021) 25082–25091, https://doi.org/10.1021/acsami.1c03283.
[192] A. Umar, M.S. Akhtar, H. Algadi, A.A. Ibrahim, M.A.M. Alhamami, S. Baskoutas, Highly sensitive and selective eco-toxic 4-nitrophenol chemical sensor based on Ag-doped ZnO nanoflowers decorated with nanosheets, Molecules 26 (2021) 4619, https://doi.org/10.3390/molecules26154619.
[193] O.C Qomaruddin, H.S. Wasisto, A. Waag, J.D. Prades, C. Fàbrega, Visible-light-driven room temperature NO_2 gas sensor based on localized surface plasmon resonance: the case of gold nanoparticle decorated zinc oxide nanorods (ZnO NRs), Chemosensors 10 (2022) 28, https://doi.org/10.3390/chemosensors10010028.
[194] C. Han, X. Li, C. Shao, X. Li, J. Ma, X. Zhang, Y. Liu, Composition-controllable p-CuO/n-ZnO hollow nanofibers for high-performance H_2S detection, Sens. Actuators B Chem. 285 (2019) 495–503, https://doi.org/10.1016/j.snb.2019.01.077.
[195] C.L. Hsu, K.C. Chen, T.Y. Tsai, T.J. Hsueh, Fabrication of gas sensor based on p-type ZnO nanoparticles and n-type ZnO nanowires, Sens. Actuators B Chem. 182 (2013) 190–196, https://doi.org/10.1016/j.snb.2013.03.002.
[196] S. Cho, D.H. Kim, B.S. Lee, J. Jung, W.R. Yu, S.H. Hong, S. Lee, Ethanol sensors based on ZnO nanotubes with controllable wall thickness via atomic layer deposition, an O2 plasma process and an annealing process, Sens. Actuators B Chem. 162 (2012) 300–306, https://doi.org/10.1016/j.snb.2011.12.081.
[197] L. Wang, H. Dou, F. Li, J. Deng, Z. Lou, T. Zhang, Controllable and enhanced HCHO sensing performances of different-shelled ZnO hollow microspheres, Sens. Actuators B Chem. 183 (2013) 467–473, https://doi.org/10.1016/j.snb.2013.03.129.
[198] H.B. Na, X.F. Zhang, Z.P. Deng, Y.M. Xu, L.H. Huo, S. Gao, Large-scale synthesis of hierarchically porous ZnO hollow tubule for fast response to ppb-level H_2S gas, ACS Appl. Mater. Interfaces 11 (2019) 11627–11635, https://doi.org/10.1021/acsami.9b00173.
[199] Y. Li, S. Wang, P. Hao, J. Tian, H. Cui, X. Wang, Soft-templated formation of double-shelled ZnO hollow microspheres for acetone gas sensing at low concentration/near room temperature, Sens. Actuators B Chem. 273 (2018) 751–759, https://doi.org/10.1016/j.snb.2018.06.110.
[200] G. Korotcenkov, B.K. Cho, The role of grain size on the thermal instability of nanostructured metal oxides used in gas sensor applications and approaches for grain-size stabilization, Prog. Cryst. Growth Charact. Mater. 58 (2012) 167–208, https://doi.org/10.1016/j.pcrysgrow.2012.07.001.
[201] A. Ponzoni, C. Baratto, N. Cattabiani, M. Falasconi, V. Galstyan, E. Nunez-Carmona, F. Rigoni, V. Sberveglieri, G. Zambotti, D. Zappa, Metal oxide gas sensors, a survey of selectivity issues, Sensors 17 (2017) 714, https://doi.org/10.3390/s17040714.
[202] A. Sáaedi, P. Shabani, R. Yousefi, High performance of methanol gas sensing of ZnO/PAni nanocomposites synthesized under different magnetic field, J. Alloys Compd. 802 (2019) 335–344, https://doi.org/10.1016/j.jallcom.2019.06.088.
[203] S. Jain, N. Karmakar, A. Shah, D.C. Kothari, S. Mishra, N.G. Shimpi, Ammonia detection of 1-D ZnO/polypyrrole nanocomposite: effect of CSA doping and their structural, chemical, thermal and gas sensing behavior, Appl. Surf. Sci. 396 (2017) 1317–1325, https://doi.org/10.1016/j.apsusc.2016.11.154.
[204] M.A. Chougule, D.S. Dalavi, S. Mali, P.S. Patil, A.V. Moholkar, G.L. Agawane, J. H. Kim, S. Sen, V.B. Patil, Novel method for fabrication of room temperature polypyrrole–ZnO nanocomposite NO_2 sensor, Measurement 45 (2012) 1989–1996, https://doi.org/10.1016/j.measurement.2012.04.023.
[205] R. Andre, D. Kwak, Q. Dong, W. Zhong, D. Correa, L. Mattoso, Y. Lei, Sensitive and selective NH_3 monitoring at room temperature using ZnO ceramic nanofibers decorated with poly(styrene sulfonate, Sensors 18 (2018) 1058, https://doi.org/10.3390/s18041058.
[206] H. Wang, Y. Luo, B. Liu, L. Gao, G. Duan, CuO nanoparticle loaded ZnO hierarchical heterostructure to boost H_2S sensing with fast recovery, Sens. Actuators B Chem. 338 (2021), 129806, https://doi.org/10.1016/j.snb.2021.129806.
[207] A. Sholehah, K. Karmala, N. Huda, L. Utari, N.L.W. Septiani, B. Yuliarto, Structural effect of ZnO-Ag chemoresistive sensor on flexible substrate for ethylene gas detection, Sens. Actuators A Phys. 331 (2021), 112934, https://doi.org/10.1016/j.sna.2021.112934.
[208] Y.H. Zhang, M.X. Peng, L.J. Yue, J.L. Chen, F.L. Gong, K.F. Xie, S.M. Fang, A room-temperature aniline sensor based on Ce doped ZnO porous nanosheets with abundant oxygen vacancies, J. Alloys Compd. 885 (2021), 160988, https://doi.org/10.1016/j.jallcom.2021.160988.
[209] Y. Tu, C. Kyle, H. Luo, D.W. Zhang, A. Das, J. Briscoe, S. Dunn, M.M. Titirici, S. Krause, Ammonia gas sensor response of a vertical zinc oxide nanorod-gold junction diode at room temperature, ACS Sens. 5 (2020) 3568–3575, https://doi.org/10.1021/acssensors.0c01769.
[210] L. Zhang, J. Zhang, Y. Huang, H. Xu, X. Zhang, H. Lu, K. Xu, P.K. Chu, F. Ma, Hexagonal ZnO nanoplates/graphene composites with excellent sensing performance to NO2 at room temperature, Appl. Surf. Sci. 537 (2021), 147785, https://doi.org/10.1016/j.apsusc.2020.147785.
[211] B.G. Ghule, N.M. Shinde, S.D. Raut, S.F. Shaikh, A.M. Al-Enizi, K.H. Kim, R. S. Mane, Porous metal-graphene oxide nanocomposite sensors with high ammonia detectability, J. Colloid Interface Sci. 589 (2021) 401–410, https://doi.org/10.1016/j.jcis.2020.12.096.
[212] E. Wongrat, T. Nuengnit, R. Panyathip, N. Chanlek, N. Hongsith, S. Choopun, Highly selective room temperature ammonia sensors based on ZnO nanostructures decorated with graphene quantum dots (GQDs), Sens. Actuators B Chem. 326 (2021), 128983, https://doi.org/10.1016/j.snb.2020.128983.
[213] A.D. Ugale, G.G. Umarji, S.H. Jung, N.G. Deshpande, W. Lee, H.K. Cho, J.B. Yoo, ZnO decorated flexible and strong graphene fibers for sensing NO2 and H2S at room temperature, Sens. Actuators B Chem. 308 (2020), 127690, https://doi.org/10.1016/j.snb.2020.127690.
[214] L. Utari, N.L.W. Septiani, S. Nugraha, L.O. Nur, H.S. Wasisto, B. Yuliarto, Wearable carbon monoxide sensors based on hybrid graphene/ZnO nanocomposites, IEEE Access 8 (2020) 49169–49179, https://doi.org/10.1109/ACCESS.2020.2976841.
[215] T. Sen, S. Mishra, N.G. Shimpi, Synthesis and sensing applications of polyaniline nanocomposites: a review, RSC Adv. 6 (2016) 42196–42222, https://doi.org/10.1039/C6RA03049A.
[216] A. Ait El Fakir, Z. Anfar, A. Amedlous, A. Amjlef, S. Farsad, A. Jada, N. El Alem, Synergistic effect for efficient catalytic persulfate activation in conducting polymers-hematite sand composites: enhancement of chemical stability, Appl. Catal. A Gen. 623 (2021), 118246, https://doi.org/10.1016/j.apcata.2021.118246.
[217] S. Li, X. Wei, C. Wu, B. Zhang, S. Wu, Z. Lin, Constructing three-dimensional structured V_2O_5 /conductive polymer composite with fast ion/electron transfer kinetics for aqueous zinc-ion battery, ACS Appl. Energy Mater. 4 (2021) 4208–4216, https://doi.org/10.1021/acsaem.1c00573.
[218] M. Usman, M. Adnan, M.T. Ahsan, S. Javed, M.S. Butt, M.A. Akram, *In situ* synthesis of a polyaniline/Fe–Ni Codoped Co_3O_4 composite for the electrode material of supercapacitors with improved cyclic stability, ACS Omega 6 (2021) 1190–1196, https://doi.org/10.1021/acsomega.0c04306.
[219] S. Cichosz, A. Masek, M. Zaborski, Polymer-based sensors: a review, Polym. Test. 67 (2018) 342–348, https://doi.org/10.1016/j.polymertesting.2018.03.024.
[220] C. Duc, M.L. Boukhenane, J.L. Wojkiewicz, N. Redon, Hydrogen sulfide detection by sensors based on conductive polymers: a review, Front. Mater. 7 (2020) 6, https://doi.org/10.3389/fmats.2020.00215.
[221] M. Tomić, M. Šetka, L. Vojkůvka, S. Vallejos, VOCs sensing by metal oxides, conductive polymers, and carbon-based materials, Nanomaterials 11 (2021) 552, https://doi.org/10.3390/nano11020552.
[222] P.P. Conti, R.S. Andre, L.A. Mercante, L. Fugikawa-Santos, D.S. Correa, Discriminative detection of volatile organic compounds using an electronic nose based on TiO2 hybrid nanostructures, Sens. Actuators B Chem. 344 (2021), 130124, https://doi.org/10.1016/j.snb.2021.130124.
[223] W. Guo, B. Zhao, Q. Zhou, Y. He, Z. Wang, N. Radacsi, Fe-doped ZnO/reduced graphene oxide nanocomposite with synergic enhanced gas sensing performance for the effective detection of formaldehyde, ACS Omega 4 (2019) 10252–10262, https://doi.org/10.1021/acsomega.9b00734.
[224] L.P. Bakos, N. Justh, U.C. Moura da Silva Bezerra da Costa, K. László, J.L. Lábár, T. Igricz, K. Varga-Josepovits, P. Pasierb, E. Färm, M. Ritala, M. Leskelä, I. M. Szilágyi, Photocatalytic and gas sensitive multiwalled carbon nanotube/TiO_2-ZnO and ZnO-TiO_2 composites prepared by atomic layer deposition, Nanomaterials 10 (2020) 252, https://doi.org/10.3390/nano10020252.
[225] N. Sebastian, W.C. Yu, D. Balram, Synthesis of amine-functionalized multi-walled carbon nanotube/3D rose flower-like zinc oxide nanocomposite for sensitive electrochemical detection of flavonoid Morin, Anal. Chim. Acta 1095 (2020) 71–81, https://doi.org/10.1016/j.aca.2019.10.026.
[226] M. Jagannathan, D. Dhinasekaran, A.R. Rajendran, B. Subramaniam, Selective room temperature ammonia gas sensor using nanostructured ZnO/CuO@graphene on paper substrate, Sens. Actuators B Chem. 350 (2022), 130833, https://doi.org/10.1016/j.snb.2021.130833.
[227] X. Chang, S. Sun, S. Sun, T. Liu, X. Xiong, Y. Lei, L. Dong, Y. Yin, ZnO nanorods/carbon black-based flexible strain sensor for detecting human motions, J. Alloys Compd. 738 (2018) 111–117, https://doi.org/10.1016/j.jallcom.2017.12.094.
[228] M.K. Mohanapriya, K. Deshmukh, K. Kumar Sadasivuni, G. Thangamani, K. Chidambaram, M. Basheer Ahamed, S.K. Khadheer Pasha, Enhanced quality factor of polyvinyl formal (PVF) based nanocomposites filled with zinc oxide and carbon black nanoparticles for wireless sensing applications, Mater. Today Proc. 9 (2019) 199–216, https://doi.org/10.1016/j.matpr.2019.02.153.
[229] M. Jian, C. Wang, Q. Wang, H. Wang, K. Xia, Z. Yin, M. Zhang, X. Liang, Y. Zhang, Advanced carbon materials for flexible and wearable sensors, Sci. Chin. Mater. 60 (2017) 1026–1062, https://doi.org/10.1007/s40843-017-9077-x.
[230] X. Chen, Y. Shen, P. Zhou, S. Zhao, X. Zhong, T. Li, C. Han, D. Wei, D. Meng, NO_2 sensing properties of one-pot-synthesized ZnO nanowires with Pd functionalization, Sens. Actuators B Chem. 280 (2019) 151–161, https://doi.org/10.1016/j.snb.2018.10.063.
[231] A. Sanger, S.B. Kang, M.H. Jeong, C.U. Kim, J.M. Baik, K.J. Choi, All-transparent NO_2 gas sensors based on freestanding Al-doped ZnO nanofibers, ACS Appl. Electron. Mater. 1 (2019) 1261–1268, https://doi.org/10.1021/acsaelm.9b00210.
[232] O. Alev, N. Sarıca, O. Özdemir, L.Ç. Arslan, S. Büyükköse, Z.Z. Öztürk, Cu-doped ZnO nanorods based QCM sensor for hazardous gases, J. Alloys Compd. 826 (2020), 154177, https://doi.org/10.1016/j.jallcom.2020.154177.
[233] O. Lupan, V. Postica, T. Pauporté, B. Viana, M.I. Terasa, R. Adelung, Room temperature gas nanosensors based on individual and multiple networked Au-modified ZnO nanowires, Sens. Actuators B Chem. 299 (2019), 126977, https://doi.org/10.1016/j.snb.2019.126977.

[234] L. Zhu, Y. Li, W. Zeng, Enhanced ethanol sensing and mechanism of Cr-doped ZnO nanorods: experimental and computational study, Ceram. Int. 43 (2017) 14873–14879, https://doi.org/10.1016/j.ceramint.2017.08.003.
[235] R. Sankar Ganesh, E. Durgadevi, M. Navaneethan, V.L. Patil, S. Ponnusamy, C. Muthamizhchelvan, S. Kawasaki, P.S. Patil, Y. Hayakawa, Low temperature ammonia gas sensor based on Mn-doped ZnO nanoparticle decorated microspheres, J. Alloys Compd. 721 (2017) 182–190, https://doi.org/10.1016/j.jallcom.2017.05.315.
[236] U.T. Nakate, P. Patil, R.N. Bulakhe, C.D. Lokhande, S.N. Kale, M. Naushad, R. S. Mane, Sprayed zinc oxide films: ultra-violet light-induced reversible surface wettability and platinum-sensitization-assisted improved liquefied petroleum gas response, J. Colloid Interface Sci. 480 (2016) 109–117, https://doi.org/10.1016/j.jcis.2016.07.010.